

Effect of Human Basement Membrane on Cardiac Tissue Regeneration after Myocardial Infarction Development of Methods

Submitted at the
Austrian Marshall Plan Foundation



AUSTRIAN
MARSHALL PLAN FOUNDATION
VIENNA | AUSTRIA

by

Alexandra-Madelaine TICHY

Area of emphasis:

Practical Training Semester at the Frank Reidy Research Center, Norfolk, VA
Cardiac Electrophysiology

Bachelor Degree Program: Medical and Pharmaceutical Biotechnology, IMC FH
Krems

Internal Supervisor: Prof. (FH) Dr. Andreas Eger

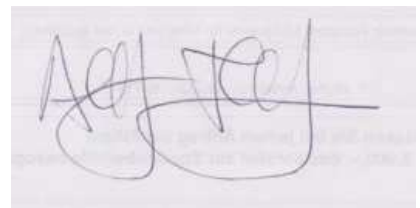
External Supervisor: Dr. Christian Zemlin

Date: March 9th, 2014

Statutory Declaration

"I declare in lieu of an oath that I have written this bachelor thesis myself and that I have not used any sources or resources other than stated for its preparation. I further declare that I have clearly indicated all direct and indirect quotations. This bachelor thesis has not been submitted elsewhere for examination purposes."

Datum: 24.02.2014



Alexandra-Madelaine TICHY

I. Abstract

With around 7 million annual deaths, coronary heart disease is the single leading cause of death worldwide¹. Myocardial infarction, also known as heart attack, is among the diseases contributing to this high death toll. Myocardial infarction describes the loss of cardiomyocytes and damage to myocardium caused by the occlusion of a coronary artery. The occlusion of a coronary artery induces ischemia, the reduced or stopped flow of blood resulting insufficient oxygen supply to the tissue. Even if myocardial infarction patients survive the initial insult, left ventricular dilation and remodeling are severe problems to consider, as they can lead to serious cardiac malfunctioning and often heart failure.

Several studies have been conducted trying to find a treatment that will improve and increase the life span of patients after myocardial infarction, for example by preventing or reducing left ventricular remodeling and increasing left ventricular function and thus cardiac output. Major accomplishments in this field have been done with the use of biomaterials, such as left ventricular restraints, in vitro engineered tissue patches or injected as scaffold with or without cells. This study aims to investigate the effect of a novel biomaterial, human basement membrane derived from donor hearts, on the regeneration of cardiac tissue after myocardial infarction.

To assess the effect of human basement membrane on myocardial infarction, a heart attack is artificially induced in rats through ligation of the left anterior descending artery and subsequent injection of the biomaterial in the infarcted area. Before and in certain intervals after the surgery, cardiac function will be assessed in vivo by echocardiography. Afterwards, voltage-sensitive optical mapping is performed on the heart to evaluate electrical activity of the infarcted and regenerated area.

This paper focuses on the development of the methods employed, as this was my main task in this study.

Table of contents

| | |
|---|-----------|
| Statutory Declaration | 2 |
| I. Abstract | 3 |
| II. Abbreviations | 5 |
| III. List of tables and figures | 6 |
| 1. Introduction | 7 |
| 2. Materials and Methods | 19 |
| 3. Results | 25 |
| 3.1. Surgical Procedure | 25 |
| 3.2. Echocardiography | 29 |
| 3.2.1. <i>Recording of Images</i> | 29 |
| 3.2.2. <i>Measurements and Calculations</i> | 30 |
| 3.3. Optical Mapping | 33 |
| 3.3.1. <i>Harvest of heart</i> | 33 |
| 3.3.2. <i>Life support system and image acquisition</i> | 34 |
| 3.3.3. <i>Signal evaluation</i> | 36 |
| 4. Discussion | 39 |
| 5. References | 47 |

II. Abbreviations

| | |
|-----|----------------------------------|
| AS | atherosclerosis |
| BP | blood pressure |
| CA | Coronary artery |
| CAD | coronary artery disease |
| CCD | charge coupled device |
| ECM | extra cellular matrix |
| EF | ejection fraction |
| HBM | human basement membrane |
| HF | heart failure |
| I.M | intramuscular |
| I.P | intraperitoneal |
| I.V | intravenous |
| LAD | left anterior descending artery |
| LSS | life support system |
| LV | left ventricle/ left ventricular |
| MI | myocardial infarction |
| PLA | parasternal long axis |

III. List of tables and figures

| | |
|--|-----------|
| Table 1: Composition of Tyrode’s solution..... | 35 |
| <hr/> | |
| Figure 1: Three different tissue engineering approaches | 10 |
| Figure 2: Different views/cross-sections used in 2D echocardiography..... | 17 |
| Figure 3 User interface of optical mapping program..... | 22 |
| Figure 4: Effects of different types of filtering on fluorescent signals..... | 25 |
| Figure 5: A-D schematic illustration of tracheostomy | 28 |
| Figure 6: Ligation of LAD and area of resulting myocardial infarction | 29 |
| Figure 7: Schematic drawing and photo of MI injection needle | 30 |
| Figure 8: Parasternal long axis view of the left ventricle | 32 |
| Figure 9: Diastolic and systolic left ventricular measurements..... | 33 |
| Figure 10: Schematic drawing of optical mapping set up | 36 |
| Figure 11: Image of stretched signal compared to activation map | 38 |
| Figure 12: Effect of parameter change on activation map..... | 39 |
| Figure 13: M-mode through parasternal short axis view of the heart | 42 |
| Figure 14: Excitation/emission spectrum of Di-4-ANEPPS | 44 |
| Figure 15: Manually and automatically created activation map..... | 46 |

1. Introduction

Coronary artery disease (CAD), sometimes referred to as coronary heart disease, is among the leading causes of death with approximately 7 million annual deaths worldwide¹. Coronary arteries (CA) are the blood vessels that supply the heart muscle with oxygen and nutrients. The main coronary arteries branch off the aorta at its root and before the arch, through openings called ostia. There are two main arteries, the left and right coronary artery, each of which further divides into smaller branches that then encircle the heart, thus delivering blood to all parts of the myocardium. One of the major diseases resulting from CAD is myocardial infarction (MI), also known as heart attack, with around 1.5 million annual cases in the United States alone². MI occurs when the blood flow in the coronary arteries is occluded, and thus some parts of the myocardium cannot be sufficiently supplied with oxygen. A consensus document by the European Heart Journal also says that the term MI “reflects the loss of cardiomyocytes (necrosis) after prolonged ischemia”³. Often, CAD and thus also MI, is caused by atherosclerosis (AS)⁴. Atherosclerosis is the term used to describe reduced blood flow in an artery caused by plaque, depositions and muscle cells that bulge into the lumen of the vessel. Additionally, endothelial cells in the affected area can stop working correctly and release higher amounts of vasoconstrictors (like endothelin-1) and lower amounts of vasodilators (e.g. nitric oxide or prostacyclin), further contributing to the reduction of blood flow. Total occlusion, however, is most often caused by the formation of a blood clot around the existing bulge or an already existing blood clot getting stuck at this bulge, which is often termed coronary thrombosis, if occurring in the coronary arteries⁴. What causes the development of AS is not yet fully understood. Previously, it was thought that passive lipid depositions were to blame, but today’s understanding leans more towards a chronic inflammatory disease driven by lipids and leukocytes, where the inflammatory reaction was in response to initial cell damage but has gotten too excessive and out of hand^{4,5}. Small reductions of vessel diameter caused by AS lesions occur in many people, but only start to become a problem when the oxygen supply cannot meet the

tissue's demand anymore. When coronary stenosis amounts to more than 80%, downstream tissue will become ischemic, insufficiently supplied with blood, while a total occlusion of the coronary artery leads to myocardial infarction⁵. After a MI, three zones can be found in the affected tissue: at the center is the necrotic zone where cells have completely died and no more polarization and thus contraction can occur. Next to that is the damaged zone where the tissue can partly polarize and adjacent to the damaged zone, the ischemic zone can be found where only repolarization is changed⁶.

In addition to the initial damage caused by myocardial infarction, the chance of congestive heart failure (HF) rises dramatically after MI⁷. Two of the main factors contributing to this development are infarct expansion and left ventricular dilation, which leads to the heart not being able to pump enough blood into the body and tissues^{5,8}. This connection also makes LV volume a powerful tool for predicting the survival of an MI patient⁷. The mechanisms by which LV remodeling is initiated are complex, but have a lot to do with changes in extracellular matrix (ECM) composition. After cardiomyocyte death, cytokines and adhesion molecules are upregulated which leads to the recruitment of leukocytes, macrophages, neutrophils and monocytes, causing a strong inflammatory response in the infarcted area^{5,9,10}. This, and the increase in wall stress¹¹, evokes hypertrophy and the activation of matrix metalloproteinases (MMP) that degrade the ECM, thus destroying the cardiomyocyte scaffold^{9,12}. Without scaffold, cardiomyocytes lose their anchorage and start to slip, inducing infarct expansion¹² and ventricular remodeling, which can be positive at first, but if too excessive turns into negative LV remodeling¹³, which increases the risk of cardiovascular fatalities¹⁴. After initial matrix degradation and decrease in cellularity in the infarcted zone, matrix cross linking is increased resulting in a dense collagen scar⁹. This all has a great influence on LV function, especially by affecting diastolic and systolic function through LV dilation^{7,15}.

Employing tissue engineering techniques as an approach for cardiac repair by elevating LV remodeling and thus treating MI patients has been gaining more and more importance over the last decade, and especially the topic of biomaterials has

become a very popular research field. For myocardial infarction treatment, there are currently three main advances in which research is being carried out (figure 1): left ventricular restraints, in vitro engineered cardiac tissue and in situ engineered tissue¹². LV restraints are biomaterial supports designed to constrain the left ventricle in such a way as to decrease the expansion of the heart and thus prevent HF due to LV remodeling^{12,13}. When speaking of in vitro engineered tissue, the talk is of so called cardiac patches which are implanted onto the heart while in situ engineered tissue is the term used to describe biomaterial scaffolds, either alone or together with cells, that are directly injected into the heart^{10,12,13}. What all three approaches have in common, however, is that they aim to either repair, create or replace lost or damaged cardiac tissue^{10,12}.

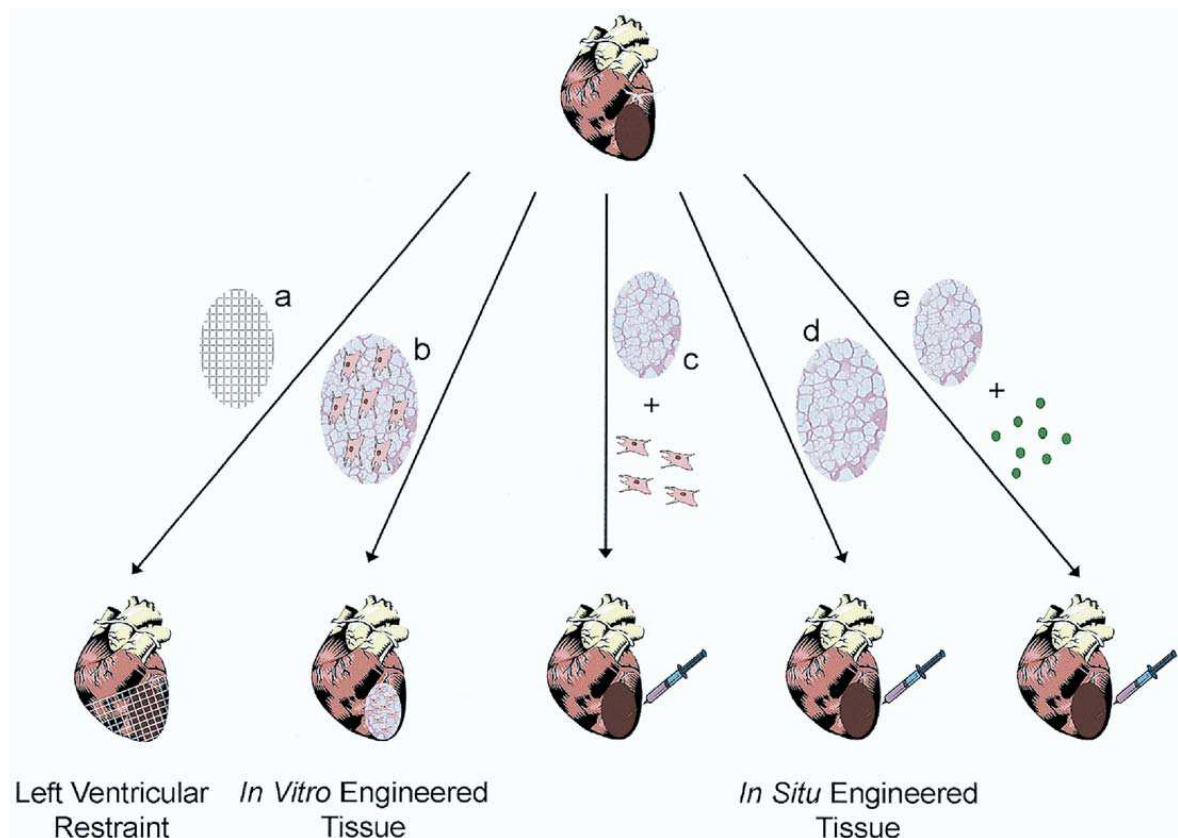


Figure 1: Three different tissue engineering approaches. (a) LV restraints; (b) in vitro engineered tissue like cardiac patches; (c-e) in situ engineered tissue in different combinations (c) biomaterial with cells (d) biomaterial by itself and (e) biomaterial with bioactive molecules.¹²

A cardiac patch is a tissue engineered biomaterial that is directly implanted onto the heart to provide stability, support cell differentiation as well as organization and also prevent anoikis¹³, cell death caused by detachment from the extracellular matrix. Originally, cardiac patches were biomaterial scaffolds seeded with cells, but recently, scaffolds alone, without any cells, have been utilized as well^{10,13}. So far, the most prevalent type of biomaterial used for cardiac patches is collagen, one of the major proteins in the extracellular matrix. This has also been tested in clinical trials, where implantation of cells together with a cardiac patch improved cardiac function more and had additional positive impacts on LV remodeling compared to therapy with cell injection alone¹⁶. Another fast advancing method in this field is the use of decellularized organ scaffolds instead of biomaterial scaffolds: whole hearts or part of the heart are decellularized with detergents, providing a scaffold that closely mimics cardiac architecture and ECM composition. This scaffold can then be reseeded with the chosen cell type to resemble cardiac compositions even more closely¹⁷. However, application of cardiac patches is limited by major drawbacks: cardiac patches often exhibit poor retention and survival of cells¹⁸ and due to limitations and difficulties in diffusion across the whole patch, it is problematic to grow patches with clinically relevant thickness (~1cm)^{13,18}. In addition to the inherent oxygen diffusion problems across the patch, the infarcted area often shows only little vascularization to begin with¹². All of this limits the contractility of the cardiac patch.

In recent years, tissue engineering research for the treatment of MI was often based on implantable scaffolds. Now, the focus and effort is shifting more towards in situ engineered solutions, which can be designed so as to be applied via a catheter, making it less invasive and thus providing a big advantage over transplantable options¹⁰. In situ engineered applications use biomaterials - by themselves, seeded with cells or mixed with bioactive molecules - which are injected directly into the infarcted area. Depending on the type of biomaterial used, different effects on cardiac tissue are pursued: repopulation of damaged area by injected cells, mobilization of progenitor or stem cells to infarction or stabilization of the extracellular matrix¹⁰. As scaffold, several different types of biomaterial have been used and studied, ranging from two component-materials such as fibrin glue

(which is formed by mixing fibrinogen with thrombin)^{19,20}, over extracellular matrix protein based materials like collagen²¹ and matrigel²² to polysaccharides such as alginate, extracted from brown seaweed^{10,23}. In animal studies, varying results could be observed: fibrin glue led to improved LV function and geometry when injected alone or with myoblasts, injection of matrigel with cells showed better results than just matrigel or just cells and alginate and collagen alone increase cardiac function and LV geometry compared to saline injection^{10,12}. Newer forms of biomaterial are artificially created, synthetic ones instead of biologically based biomaterials. Synthetic biomaterials offer the advantage of controllable properties like degradation, stiffness, porosity or gelation time and also the problem of variations from batch to batch is no longer a concern¹³. The results of a computer simulation investigating the effect of material injection into the infarcted myocardium suggest that the injection of biomaterials of adequate density and stiffness alone (without any cells) could be sufficient to have a positive effect on LV remodeling²⁴. The hypothesis is that the wall stress on the LV can be reduced by increasing the LV wall thickness^{13,24}, according to Laplace's law which says the wall stress is indirect proportional to two times the wall thickness²⁵. In practice, however, the result was not quite the same: injection of a synthetic, non-degradable polyethylene glycol (PEG) hydrogel in rats post MI did lead to an increase in wall thickness, but the pathological progression of the infarction was similar to that of saline treated animals¹³. This suggest that successful MI treatment with biomaterial injection may be linked to the inherent bioactivity and degradable properties of biomaterials, which are important factors for allowing cellular infiltration of the biomaterial^{13,18}.

Besides the various types of biomaterial scaffolds, several different cell types have been used as well, and each has advantages and disadvantages. Commonly used cells are skeletal muscle-derived progenitors (myoblasts)^{26,27} or crude bone marrow mono-nuclear cell sheets^{10,20}. The advantages of these cells are that they are readily available, can be derived from the patients themselves and are easily grown in vitro. Their disadvantage is that they have poor transdifferentiation abilities when injected¹⁰. An alternative is provided by bone-marrow derived

mesenchymal stem cells²⁸, which are starting to be more popular because of their higher efficacy, but use is still limited due to the low recovery yield from tissue¹⁰.

Typically, biomaterials have been used as scaffolds for cells or by themselves. However, biomaterials are now also often used as vehicles for other bioactive molecules, such as genes or proteins which in turn are stimulating tissue regeneration^{12,13}. Binding of the bioactive molecule to the scaffold can prolong the release, and with present day engineering possibilities, the biomaterial can be designed in such a way as to facilitate even more effective molecule releases. Furthermore, attachment to the biomaterial may enhance the activity of certain proteins, e.g. growth factors, since they are usually ECM bound proteins¹⁸.

This study is investigating the effects of a novel biomaterial, human basement membrane, derived from human donor hearts. Basement membrane is a 100-300nm thick membrane that underlies all epithelial cells and, in higher developed organisms, can also surround endothelial cells, nerve cells, smooth muscle cells or adipocytes²⁹. It is formed during embryonic development from embryonic epithelium and is mostly made up of proteins, glycoproteins, proteoglycans, nidogens and perlecans^{29,30}. The main components of the basement membrane are laminin and type IV collagen, which are also the only constituents that have the ability to self assemble into polymers³⁰. Both collagen IV and laminin comprise several different subunits which can form heterotrimers to make up the polymer structure, the distribution of those subunit chains being tissue specific^{29,31}. Additionally, basement membrane also contains different matrix bound growth factors and adhesion receptor ligands that have supporting and regulatory influence concerning structure and function on the surrounded cells^{29,31}. Even though the rather small pore sizes of basement membranes allow only very small molecules to diffuse across it, cells still have to the ability to migrate very rapidly by employing tissue invasive actions such as activating matrix-metalloproteases that degrade the ECM²⁹. Basement membrane is very similar to another biomaterial called Matrigel. Matrigel is a sterile protein mixture extracted from Engelbreth-Holm-Swarm (EHS) mouse sarcomas that closely resembles basement membrane with respect to growth factor and macromolecule

composition, and forms a 3D gel at physiological temperatures^{22,32}. Matrigel as a MI treatment option has been frequently investigated in animal studies, with encouraging results^{22,33}. Some of the possible mechanisms are: providing structural support which helps preventing or reducing LV remodeling, creating an environment that encourages cell survival AND functioning (through growth factors), inducing neovascularization, supplying ischemic tissue with additional nutrients and thus increasing proliferation, and providing a suitable microenvironment for stem cells²². This has also been tested in vitro, where stem cells plated on matrigel have been cultured into functioning, beating cardiomyocytes³⁴. We hypothesize that injection of human basement membrane will have at least similar results on myocardial infarction treatment, but with more advantages. Despite successful animal studies with matrigel, the translation to human clinical trials and applications may be questionable, due to the mouse sarcoma origin, which will always pose the threat of uncontrollable cell or tumor growth in the patient. This assumption is strengthened by the fact that no clinical trials have yet been conducted, even though matrigel used in various fields for more than 30 years³². As the human basement membrane used in this study is derived from human donor hearts in a sterile manner, the translation to clinical studies should prove much easier and safer. Also, the fate and behavior of a cell is, to a high degree, determined by the surrounding microenvironment, of which the ECM is a big part of. The molecular composition, density and stiffness thus have a great influence on cells and therefore also on an individual's health³¹. As mentioned earlier, especially the composition of laminin and collagen IV polymers is tissue specific^{29,31}, so the human heart origin should result in an ECM composition, especially with respect to laminin and collagen IV, more similar to the natural cardiac ECM than the mouse sarcoma derived matrigel. Furthermore, even though a stem cell niche in cardiac tissue is still very unknown and uncharacterized, resident cardiac stem cells (CSC) are thought to be quiescent in the adult cardiac tissue and only engage in repair functions when activated^{31,35}. Since HBM is already derived from hearts, the chances of providing the right microenvironment for CSC activation are higher.

In order to test any treatment option of MI, a suitable test model needs to be found. Not only are there different ways of inducing an MI with varying outcomes, but also considerations concerning species and strain of the animal model need to be made. For the induction of left ventricular myocardial infarction, various techniques have been used, all through the (partial) occlusion of the left coronary artery or branches of it, like the left anterior descending (LAD). One method to cause myocardial infarction is through induction of AS. This can be achieved through feeding the model animal a fat/cholesterol rich diet and thus causing hypercholesterolemia³⁶. Even though AS and subsequent MI was developed in several different animal species through this method, the time and place of occurrence was very unpredictable and variable, thus making it not very suitable for experimental studies³⁶. Another way of achieving occlusion that had been in use in the early days of myocardial infarction studies is through electrocauterization or causing diffuse necrosis by administration of subcutaneous isoproterenol³⁷. However, today's most employed method of MI induction is by surgical occlusion, through special occlusion tools, balloon inflation in the artery or ligation with suture: these provide precise, and above all, reproducible ways of inducing myocardial infarction³⁶.

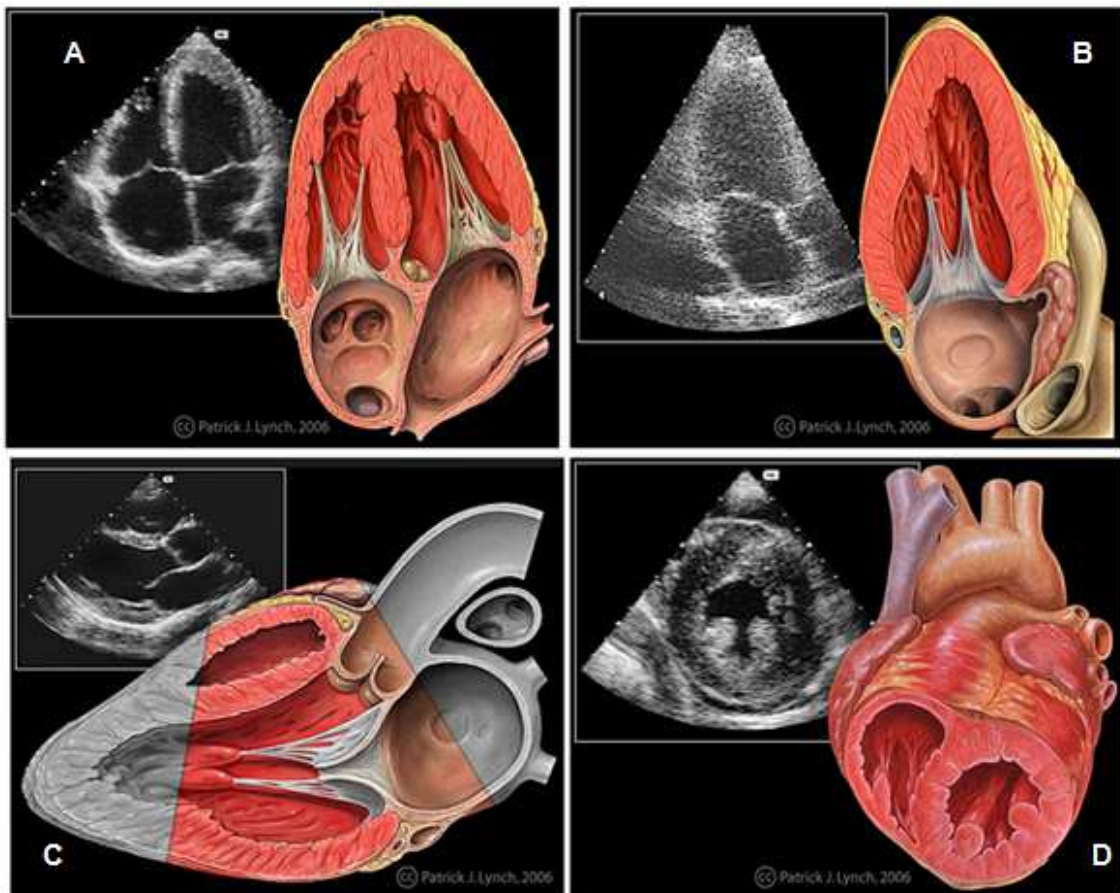
Besides deciding on the right induction approach, it is important to decide on the most suitable animal model. Even though the induction of MI itself is possible in a variety of animals, it is important to ensure that the pathophysiology is rather similar to the clinical condition in patients. Especially for studies of similar scale as this one, the use of rodents has proven very advantageous, most of all rat models. The most striking advantage of using rats is that the progression of heart failure after MI resembles the progression in patients very closely: after survival of the initial MI, no further ischemic insult is needed for HF to develop, because the myocardium of both rats and humans is unable to sufficiently compensate for the lost or damaged tissue function³⁸. Furthermore, the course of ventricular remodeling in rats is comparable to that in humans. First, the infarcted wall area begins to thin before scar formation occurs, while the non-infarcted myocardium goes into hypertrophy in response to additional wall stress^{38,39}. Even the histological development of this process is similar³⁹. And not only is the

pathophysiological progression itself rather similar, also the response of rats to pharmacological treatments has been a good tool for the prediction of patient response to the same treatment³⁸. Another asset of rats is their relatively low cost per animal and for housing, which allows for more numbers in a study and thus higher statistical relevance^{37,38}. Furthermore, progress has been made in the field of echocardiography which allows for better assessment of cardiac function even in small animals like rodents³⁷. Apart from all these obvious benefits, it also advantageous that the myocardial infarct model in rats has been studied and characterized so extensively. So has today's widely used model of coronary artery ligation in rats been developed by Pfeffer et al.³⁹ already in the 1970s³⁷, and soon after that, in the 70s and 80s, the structural, functional and biochemical changes after CA ligation have been closely studied³⁸. It was also around that time that the relation between infarct size and chamber dilation and function was shown^{37,39}. The usefulness of the rat MI model has also been proven by the utilization of it in many groundbreaking studies. For example, early studies of the angiotensin converting enzyme captopril have been conducted in rats, the promising results of those leading to the SAVE clinical trials⁴⁰. Also, the function of angiotensin II type 1 receptor antagonists on LV structure and function after MI has been tested first in rats³⁷.

For the assessment of MI treatment efficacy, different diagnostic methods are available. In cardiovascular research, often the left ventricular parameters such as geometry and pressure have been used. In earlier MI studies, the traditional criterion for subsequent heart failure was left ventricular end diastolic (LVED) pressure, because it reflected the preload⁴¹. However, for this method, it was necessary to cannulate the carotid artery and catheterize the LV, which made it rather unsuitable for the observation over a longer period of time, and also the catheterization could cause possible damage to the aortic valve as well as affect cardiac performance⁴¹.

A less invasive alternative to LVED measurement is provided through echocardiography, a type of sonography. In sonography, a transducer head is applied to the skin where it emits ultrasound waves (sound waves with a frequency

higher than 20 kHz) that are able to travel through tissue. Upon contact with tissue, the ultrasound is echoed back. A computer collects all the reflected sound waves, and is able to generate an image of the underlying organ structure by evaluating the intensity of the reflection and how much time elapsed until the reflected waves were then detected. Echocardiography specifically describes sonography employed for imaging the heart. Because echocardiography is non-invasive and has no known side effects, even after very frequent use⁴², it has



become a commonly used option in cardiovascular studies. In humans, it has been
Figure 2: Different views/cross-sections used in 2D echocardiography. (A) Apical 4 chamber view, transducer is placed at the apex of heart and all 4 chambers are visible. (B) apical 2 chamber view, transducer is placed at the apex of heart and only two chambers are visible. (C) parasternal long axis, transducer is placed beside the sternum and along the long axis of the heart/ventricle. (D) parasternal short axis vies, transducer is placed beside sternum and along short axis of the heart. Modified after⁶⁰

a well-established technique for a long time, but has only in the last two decades gained popularity in small-rodent research, despite the rat being such a common model for this type of research⁴³. The main reasons for this lay in the small hearts and the fast heart rate, which made it difficult to obtain images of adequate quality.

For echocardiography in rats, the region of interest is in approximately 20mm depth, which proved to be difficult because ordinary echocardiography equipment had their focus much deeper and the frame rate was not high enough to get satisfying images of the cardiac cycle⁴¹. Newer ultrasound machines have been developed with a focus on rodent research, and those machines employ high frequency vessel transducers in order to image at lower depths, and even though the rate of frames is still an area worth improving, it allows for sufficient echocardiographic images⁴¹. Besides being non-invasive and without apparent side-effects, echocardiography has different modes that can be employed, and thus making it easy to find the right variable that needs to be measured for the study at hand.

The most often used modes in echocardiography are B-Mode, M-Mode, and Doppler echocardiography. B-mode is short for brightness-mode and provides a two dimensional image of the heart, while M-mode, the motion mode, only supplies one dimensional images by visualizing one section of the two-dimensional image⁴⁴. In B-mode, the image seen is a real-time image of the selected area whereas M-mode displays tissue motion over time. For these modes, different views can be employed depending on the position of the transducer head (see figure 2). Doppler imaging is slightly different to the two previously mentioned modes, in that it does not image tissue but measures the velocity and direction of moving liquids, such as blood, by making use of the Doppler Effect⁴⁵. If a sound wave is reflected by a particle, the frequency of the wave changes depending on whether the particle was moving towards or away from the wave source, which makes it possible to determine the velocity of the fluid⁴⁵. The apparent selection of measuring modes also allows for several different variables and parameters to be measured. Some of them are LV inner diameter, area and volume (all in diastole and systole), fractional shortening (FS), ejection fraction (EF), the mitral inflow velocity and many more. This range is another advantage that makes echocardiography such an appealing method for the assessment of cardiac function.

Depending on the kind of treatment to be investigated, it is also interesting to not only assess cardiac function and the improvement thereof, but also the actual area of myocardium that is still able to excite and thus contract. As this study is based on the hypothesis to at least partly cause cardiomyocytes or stem cells accumulation in the infarcted area, the integration of those cells in the activation cycle is of special interest. In order to do this, optical mapping is performed on the rat heart. Optical mapping of the heart makes it possible to visualize different parameters as a function of time with the use of fluorescent dyes⁴⁶. In order to perform optical imaging, first a heart or tissue preparation suitable for the study needs to be found. These can range from single cells or tissue⁴⁷ to whole heart preparations like the Langendorff-perfused heart⁴⁸. After choosing the right cardiac preparation, the next important choice lies on the parameter to be studied. Among the most important and most studied ones are transmembrane voltage V_m and intracellular Calcium concentration $[Ca_i]$, but also visualization of other parameters such as pH, nitric oxide, oxygen tension or intracellular concentration of various other ions can be done^{49,50}. In accordance with the chosen parameter, the heart preparation is stained with a suitable fluorescent dye. Afterwards, the heart will be illuminated with a light source of appropriate wavelength and intensity to excite the dye, and the emitted fluorescent light is collected with a camera or sensor⁴⁶. If a change in the parameter occurs, for example the calcium concentration rises or the transmembrane voltage changes, the intensity of emitted light or the emission spectrum changes, depending on the dye used and the mechanism it employs^{49,51}. Before light reaches the sensor, it passes through a filter that ensures that only light of the emission wavelength is collected and evaluated.

2. Materials and Methods

For studying the effect human basement membrane has on cardiac regeneration and function, following procedures and evaluation methods are performed: surgical induction of MI and injection of HBM or saline; echocardiographic assessment before, 4 and 8 weeks after MI induction; and optical mapping of the perfused heart after 8 weeks. Described below are the methods used to develop the final procedures.

2.1. Development of surgical procedure

For the development of surgical procedure as in use now, nine rats of no particular strain or sex have been used. All surgeries have been conducted in accordance with the guidelines of The Institutional Animal Care and Use Committee (IACUC) of Old Dominion University. All initial procedures and subsequent changes have been approved by the IACUC. The surgical procedure described in the ODU IACUC protocol 12-020 was the basis for the first surgery, and appropriate changes have been made after each surgery. The initial procedure looked as follows:

Before surgery, the rat is anesthetized with 2% Isoflurane and the chest is shaved and disinfected. 5mg/kg Carprofen (Pfizer), as pain and inflammation treatment, are given before surgery and once per day afterwards until no signs of pain or distress are exhibited. An intraperitoneal (I.P) injection of 10-12mg/kg of the anti-arrhythmic drug Amiodarone (Hikma Pharmaceuticals) is administered right before the procedure. An orotracheal intubation is performed and intravenous (I.V.) catheter is placed in the jugular vein. Then, the anti-hypotensive drug Phenylephrine (I.V., 2-4 mg/kg or as needed to adjust blood pressure, West-Ward) is given. The antispasmodic drug Lidocaine (Hospira) is administered as a continuous drip (2-5 μ g/kg/min) throughout the whole surgery. To access the heart, a midsternal thoracotomy is performed and the LAD is permanently ligated. The rat is anesthetized for another two hours, after which 250 μ l of human basement membrane or saline are injected in the infarcted region. Afterwards, the ribs are closed, the lungs inflated by sucking out air of the thorax via a catheter and the

chest fully closed in two layers (muscle and skin). Isoflurane concentration is slowly decreased to ensure spontaneous breathing of rat before ventilation is terminated. Throughout the whole procedure, blood pressure, heart rate (ECG) and pulse-oximetry readings will be observed and collected. After each of the nine surgeries, possible ways of improvement were sought and discussed. According to that, different types of changes, from adding and omitting different drugs over change of the surgical procedure to usage of different equipment, have been implemented.

2.2. Development of echocardiography procedure

As no echocardiography protocol had been in place, a new one had to be established. This was done by researching several echocardiography procedures used by other groups, comparing them with the data needed in this study and then developing an own protocol appropriate for the experience level of the personnel conducting the ultrasound and the machinery at hand. The ultrasound machine used was the Visual Sonics Vevo 770 system capable of high frequency ultrasound imaging specific for small animal research. With the Vevo 770, B-mode and Doppler-mode imaging is possible. Technically, operation of M-mode on this system is possible but was not installed on this particular machine, and buying the software was out of this study's budget, which is why measurements had to be restricted to two dimensional imaging modes. The three different scan heads on hand were: RMV704 (20-60MHz), RMV708 (22-83MHz) and RMV716 (11-24MHz). Only the latter scan head, RMV716, was able to provide high resolution images at the needed tissue depth for rat cardiac imaging (between 10-30mm). As possible cardiac views, parasternal long (PLA) and short axis as well as apical 2 and 4 chamber views were at choice. Due to difficulty of acquiring apical view images, mostly caused by the rather large scan head, parasternal long axis view of the left ventricle was chosen as the main view. The Vevo770 provides a way of directly calculating certain parameters simply by measuring certain lengths and areas in the correct view, but the choices suitable for this study were unsatisfactory. Thus, by researching more echocardiographic protocols, the right

calculations for the needed parameters were collected and are now being calculated manually with measurements taken also manually from the obtained parasternal images.

2.3. Development of optical mapping procedure

The optical mapping procedure as is has already been in use at the cardiac electrophysiology lab of Dr. Zemlin for studying and mapping action potentials and calcium transients in mice, rats, and rabbits. No changes had to be made to the already established heart extraction surgery or the optical mapping protocol. Due to some problems in optical mapping experiments unrelated to this study, all tubes have been replaced and all stock solutions, dye or otherwise, made new.

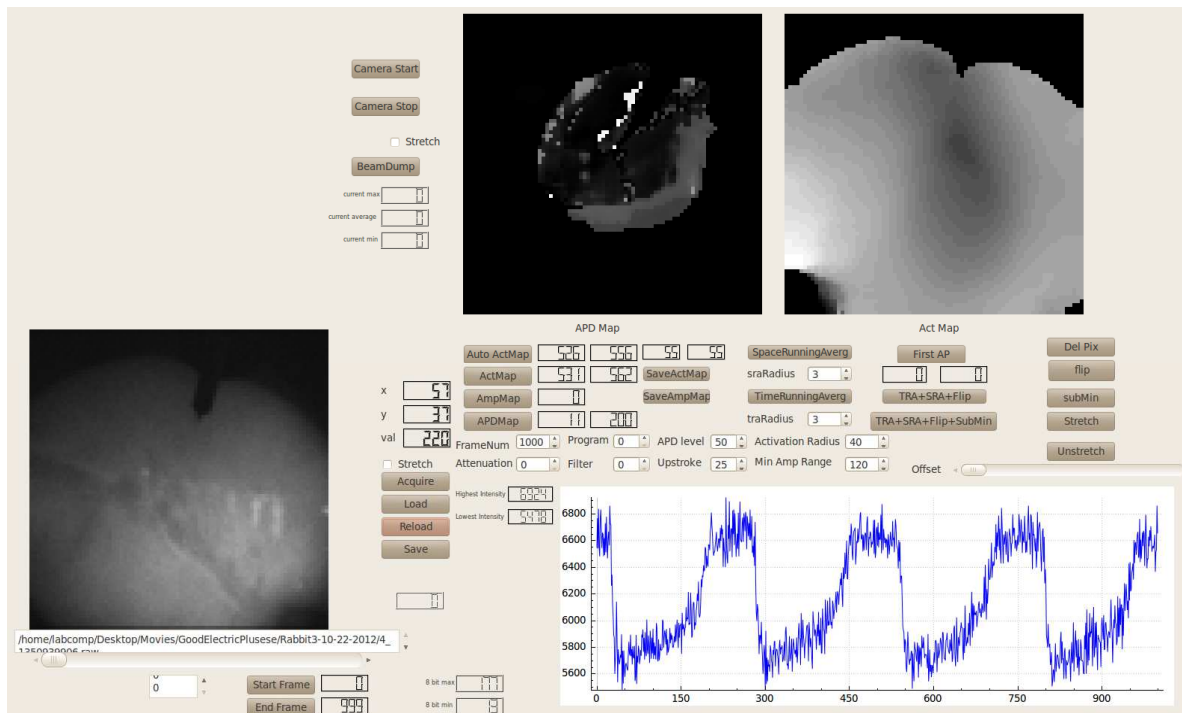


Figure 3: User interface of optical mapping program. The image on the lower left is the image as recorded by the CCD camera. The two imaged on the upper right are the Action Potential Duration (APD) and Activation maps (Act Map). The graph on the bottom shows the unfiltered fluorescent signal, with the intensity on the y axis and frame number on the x axis.

For the evaluation of the recorded data, a program written by PhD and other students working in the cardiac electrophysiology lab is being used. The program was written with the cross-platform application framework Qt Creator in the programming language C++. A screenshot of the user interface of this program

can be seen in figure 3. The three images seen on this screenshot are the image as recorded by the charge coupled device (CCD) camera (lower left), an activation potential duration (APD) and an activation (Act) map (top left and right, respectively). The signal seen in the graph is an unfiltered fluorescence signal from one of the pixels from the image on the lower left.

The program displays the image of the heart as recorded by the CCD camera. Furthermore, one can select any pixel of the image and the fluorescent signal of this pixel is shown in a graph with respect to time. The raw fluorescent signal can then be modified in several ways. The modifications mostly used are: averaging over time, averaging over space, subtracting the minimum intensity to get rid of background fluorescence and flipping of the signals. The flipping leads to display of action potentials as a positive upstroke rather than decrease of signal intensity. The thus filtered signal can further be stretched to result in higher signal intensities. By going through the frames of the stretched image, the activation propagation can be observed. The different types of filtering and the effect they have on the signal and the output image can be seen in figure 4. Another important tool in this program is the creation of an activation map. An activation map is basically a static depiction of the propagation of an action potential across the heart. In a healthy heart, the activation of myocytes starts at one point, the SA-node, and travels across the heart in a waveform as the one cell after the other gets activated. In terms of fluorescent signal, activation is shown as a drastic upstroke of intensity. Since the activation propagates and does not happen simultaneously across the heart, this drastic upstroke happens at different times for each pixel. In an activation map, the time point (=frame) at which this happens is determined for each pixel. Every pixel is then assigned a grayscale color according to this frame number – pixels where activation occurs earlier are darker and whereas pixels that are activated later are lighter. An example for an activation map can be seen in figure 3, top right image.

Previously, the creation of an activation map with this program required a lot of manual work. To determine the frame of activation for each pixel, one had to look at the filtered signal and select the frame range of an upstroke that seemed

suitable. The program then only screened pixels for activation upstrokes in this frame range. In order to improve the creation of activation maps, I rewrote the program so that the process is automated and more adaptable.

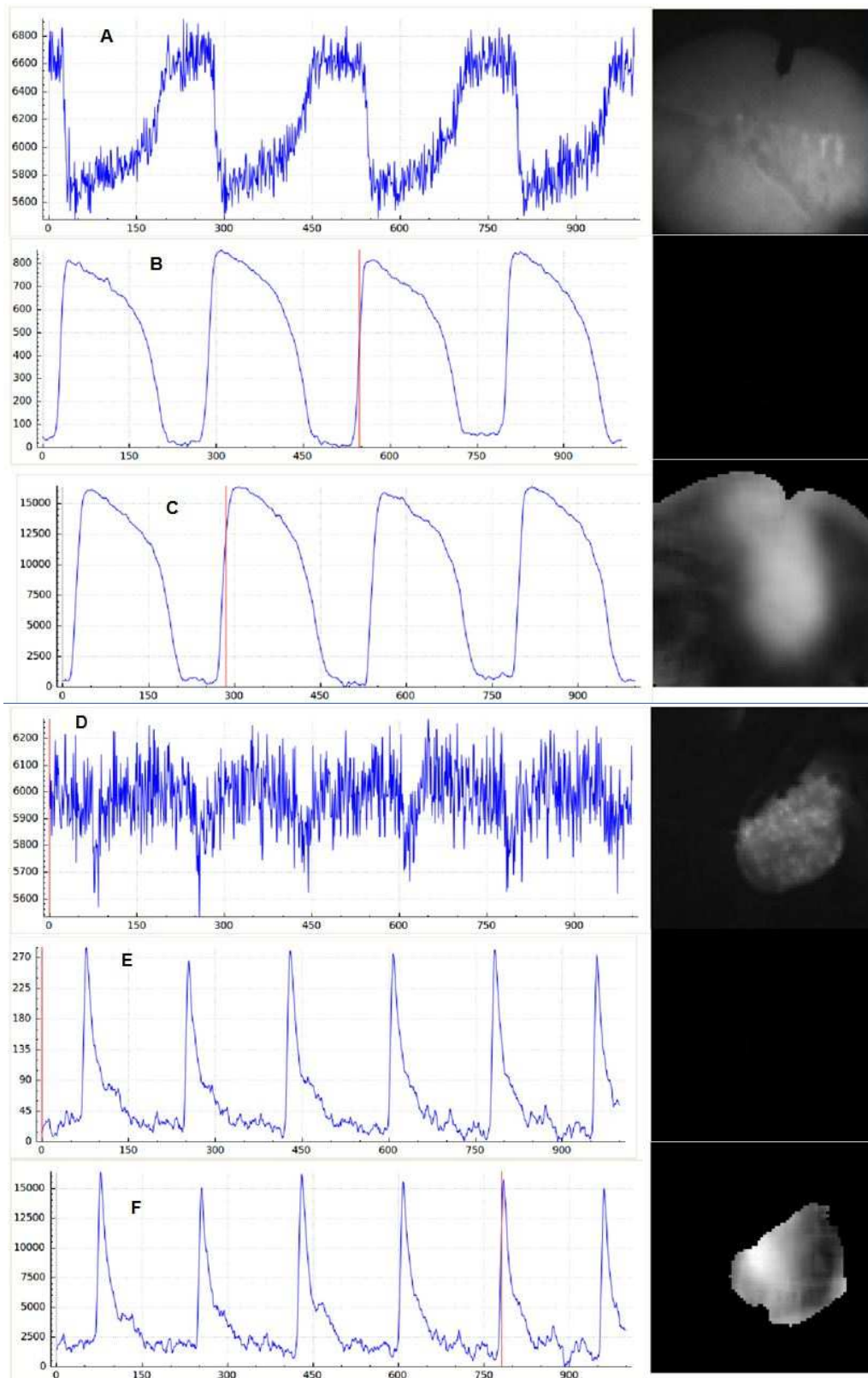


Figure 4: Effect of parameter change on activation maps Images show the effect of changing the minimum amplitude range and the activation radius. **(A)+(B)** rabbit heart. **(C-E)** mouse heart. **(A)+(B)** have the same activation radius, but in **(A)** the minimum amplitude range is higher, thus excluding more pixels. **(C)+(D)** share the same minimum amplitude range, but in **(C)** the activation radius is much wider. **(D)+(E)** have the same activation radius, but the minimum amplitude range is 60 in **(D)** and 59 in **(E)**.

3. Results

The objective of this study is to assess the potential of human basement membrane as myocardial infarction treatment. This is done by injecting the biomaterial into the infarcted area and determining the effect it has on cardiac function in different ways. The employed methods in this study are: a rat survival surgery, where a MI is induced and HBM is injected; evaluating the cardiac function via echocardiography; and determining the electrical activity of the infarcted and non-infarcted area with optical mapping. This report focuses on the development and final protocol of these, as this was my main task.

3.1. Surgical Procedure

The surgical procedure is necessary to induce MI in the rat and inject HBM or saline into the infarcted area. Over the course of nine surgeries, following changes have been made:

- Addition of the preanesthetic Ketamine (75mg/kg, Bionichepharma) and the sedative Midazolam (5mg/kg, Akorn) to reach a deeper state of anesthesia than reachable by Isoflurane and to simplify the intubation procedure. This was again decreased to injecting $\frac{1}{4}$ or $\frac{1}{2}$ of the initial amount, only when needed to reduce factors that could contribute to animal death after an animal died without clear explanation.
- Place for I.V. catheterization was reconsidered, as jugular vein proved too small and impractical. Femoral vein and a tail vein were considered, but neither one was a possible alternative, so I.V. catheterization was left out and any I.V. drugs from then on administered I.P.
- Midsternal thoracotomy (or sternotomy) was changed to left thoracotomy which provided better access to the heart. First, the 3rd intercostal space was determined as the entry point. This did not always provide the best view of the heart or the lungs were in the way, therefore the intercostal

space to be used is determined by placing the finger over the intercostal spaces and using the one where the heart beat is felt strongest.

- The vital sign monitor (DRE Waveline EZ Portable Patient Monitor) planned on being used was not able to provide good enough ECG readings to be of use. Therefore ECG readings are created with the use of an amplifier and an oscilloscope. Regular alligator clips are used as electrodes and are placed at the base of the two front limbs and one hind leg. The electrodes are then connected to an amplifier capable of capturing and amplifying input signals on levels as low as microvolts. The output signal is then transmitted to an oscilloscope, where the signal is displayed as ECG wave lines.
- The monitor was also not capable of measuring the rats' blood pressure (BP) due to the high heart rate. A lot of time has been invested in trying to find better suited blood pressure systems, but any rodent specific systems exceed this study's budget. The use of different blood pressure cuffs alone did not improve the BP readings, and self made blood pressure transducers did not provide signals that can be used during surgery. Therefore, the BP reading is not being performed.
- The drugs Amiodarone and Phenylephrine are not administered anymore. This has several reasons: Both drugs affect the BP, and without constant monitoring of the BP, there is no way of knowing how the drugs need to be counterbalanced (Amiodarone is antiarrhythmic but lowers the BP, Phenylephrine raises it again); no I.V. line is present, so Phenylephrine is administered I.P. and the time it takes to be in effect is not known. No negative effects have been observed after leaving the drugs out the first time, therefore we are continuing to leave them out to avoid unnecessary drug administration that could lead to unforeseen complications.
- Orotracheal intubation proved to more complicated than anticipated and several animals died due to wrong intubation when the intubation tube was thought to be in the trachea but was actually in the esophagus. Therefore,

the intubation procedure was changed to tracheostomy, where the intubation tube is inserted directly into the trachea (figure 5).

:

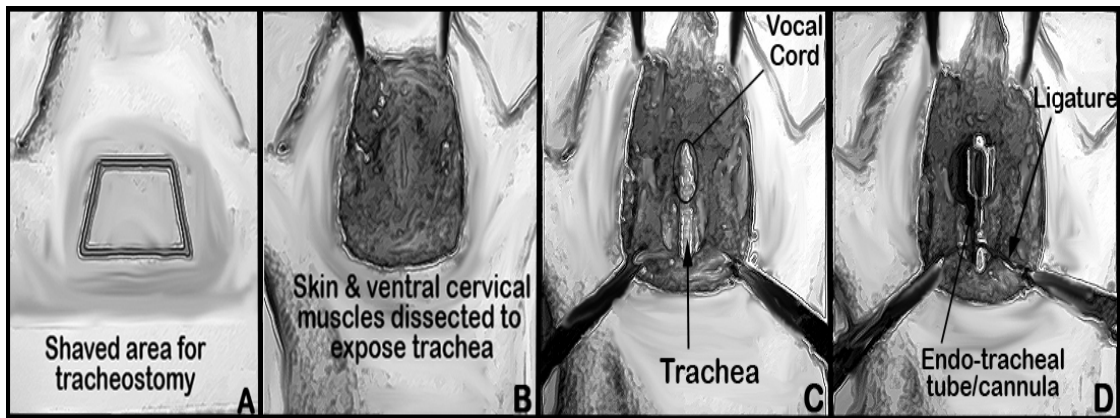


Figure 5: A-D schematic illustration of tracheostomy. Trachea is exposed and endo-tracheal tube is directly inserted into trachea through a small incision.⁶¹

The below described protocol is for the surgical procedure as in use now, after implementation of all changes.

Pre-surgery, the rat is anesthetized with ~2% Isoflurane and shaved around the chest and limbs. Then, the rat is placed on the surgical table with an extra heating pad on it, to keep the animal's body temperature from getting too low. Electrode gel is put on the ECG electrodes which are then placed on the skin near the two front paws and the left hind leg. The pulse-oxometry clamp is placed on one of the hind paws, and the temperature probe is inserted in the rectum. An I.P Lidocaine drip is started (0.3 ml Lidocaine in 150 ml saline) at approximately 1 drip in 20 seconds. This rate is adjusted throughout the procedure per surgeon's request. The shaved area of the rat is wiped down with ethanol to disinfect it. From this point on, the procedure is conducted in sterile conditions. Via a tracheal cut down, also called tracheostomy, and the rat is intubated and connected to the ventilator (Harvard rodent ventilator). The start tidal volume is set to 1.5ml at approximately 80 breaths per minute, but can be adjusted in response to O₂ saturation or if lungs are found to be inflating insufficiently during the procedure. The rat is turned on its right side, and left thoracotomy is started. The most suitable intercostal space to be used is determined by placing a finger on the animal's left side and feeling for the strongest heartbeat. In case the rat is showing signs of reaction (e.g. nerve

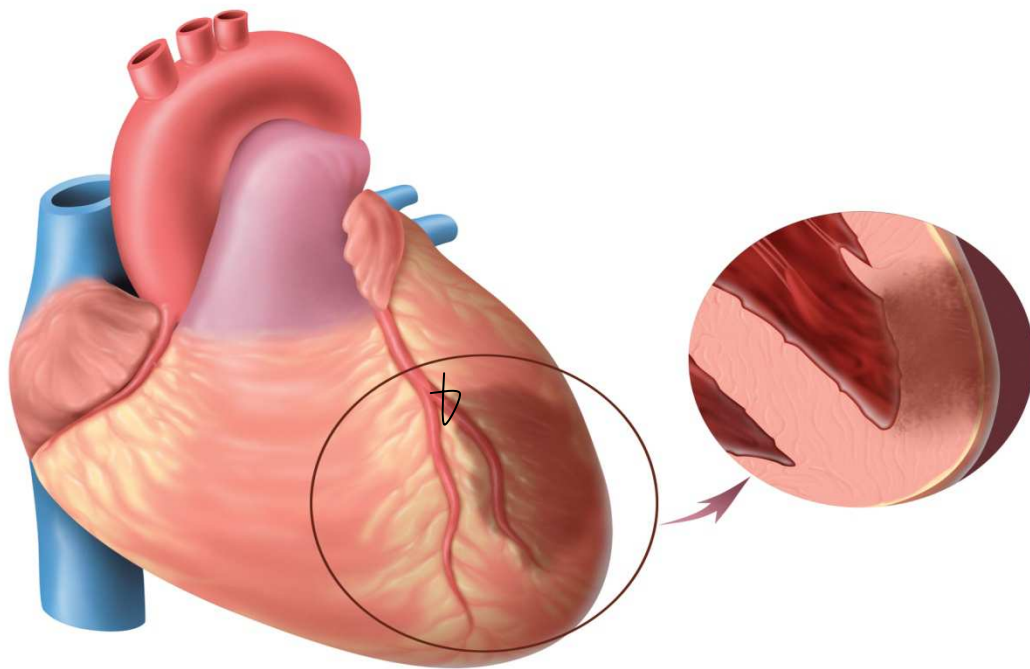


Figure 6: Ligation of LAD and area of resulting myocardial infarction. The area supplied by the occluded artery is undergoing ischemia and will eventually result in tissue loss and myocardial infarction.⁶²

twitching) during the surgery, 0.25 ml of Ketamine are administered to provide deeper sedation. Once the thoracic cavity is opened, the LAD is permanently ligated to induce myocardial infarction (figure 6) with 6-0 silk suture. After ligation, the ECG should show an elevated ST-segment. To avoid arrhythmias or in case of premature ventricular contractions, a 0.1 ml Lidocaine bolus is administered I.P. A 0.1 ml epinephrine bolus can be injected directly into the heart if signs of cardiac arrest, dysrhythmias or a general slow heart rate are seen. The thorax is then covered with wet cotton gauze to keep heart and lungs from drying out. After a waiting period of 45 minutes, 75µl of saline or HBM are injected into the infarcted area. This is done with the specially prepared needle seen in figure 7. After the injection the chest is closed. First, the intercostal space is closed by sewing the ribs back together, followed by the muscle and skin layer. During the procedure of closing the chest, the Isoflurane concentration is slightly decreased. When the rat has regained enough of its consciousness, the intubation tube is disconnected from the ventilator to ensure spontaneous breathing of the animal. If this is the case, the endo-tracheal tube is taken out, the trachea is closed and the muscle

and skin layer are sewn back together. During this time, the animal is being anesthetized with Isoflurane via a nosecone. Carprofen is administered intramuscular (I.M.) and the rat is monitored until full consciousness is regained. For the following days, rat is fed Carprofen in tablet form (2mg/tablet, Bio-Serv), one tablet a day until it exhibits no more signs of pain.

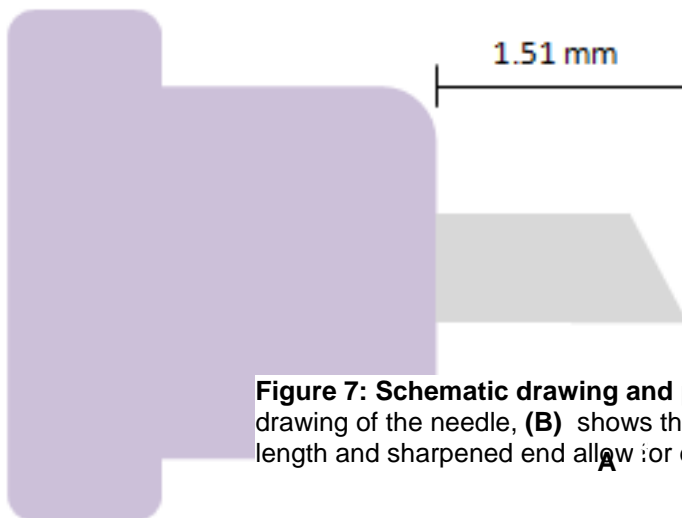


Figure 7: Schematic drawing and photo of MI injection needle. (A) shows a schematic drawing of the needle, (B) shows the shortened needle next to an unaltered needle. The short length and sharpened end allow for easy injection into the myocardium.

3.2. Echocardiography

Echocardiography is used to appraise cardiac function after myocardial infarction and subsequent HBM or saline injection. This is done by recording ultrasound images, measuring certain lengths and areas from these images and using these measurements to calculate previously determined cardiac parameters. The following procedure is used a few days before the surgery, 4 weeks post MI and 8 weeks post MI.

3.2.1. Recording of Images

Before the ultrasound assessment can be performed on the rat, the area of interest needs to be free of hair. During the whole procedure of shaving and acquiring ultrasound images, the rat is kept under anesthesia with 1.5-2%

Isofluorane. It is then shaved generously around the chest and sides. After the rat is shaved, depilatory cream is applied on the shaved area to get rid of any residual hair. Caution has to be taken to remove the cream with sufficient amounts of water before it starts to damage the animal's skin. To keep the body temperature from falling while under anesthesia, the rat is placed on a heating pad in a supine position. Generous amounts of ultrasound gel are applied to the shaved area. As scan head, the RMV 716 is used. To acquire the images of the heart in the desired view, parasternal long axis view, the scan head is placed beside the sternum in an almost parallel manner and rotated in such a way to get a long axis view of the left ventricle. Now the scan head is moved from left to right until the left ventricle is at its largest. In this view, the left atrium and aorta should be visible (figure 6). To keep the image from distorting the scan head can be placed in a special mount where it is locked in the right position while the images are recorded. 100 frames are recorded for one movie, with a frame rate of 40 frames per second.

3.2.2. Measurements and Calculations

All measurements are taken from parasternal long axis views, in diastole and systole. Diastole was defined as the time when the LV was the largest, systole when the LV was at its smallest. Following measurements were made with the program ImageJ, where lengths and traced areas can be directly analyzed.

$A_{d/s}$ left ventricular inner area diastole/systole [mm²]

$L_{d/s}$ left ventricular long axis diastole/systole [mm]

With these measurements, following calculations are made^{44,52}:

$S_{d/s}$ left ventricular short axis diastole/systole [mm]

Volume_{d/s}left ventricular volume diastole/systole [mm³]

EFejection fraction [mm]

$$S_{d/s} = \frac{4 \cdot A_{d/s}}{L_{d/s} \cdot \pi}$$

$$V = 0.85 \frac{(A_{d/s})^2}{L_{d/s}}$$

$$EF = \frac{V_d - V_s}{V_d} * 100$$



Figure 8: Parasternal long axis view of the left ventricle. In this view, left ventricle (LV), left atrium (LA) and the aorta are visible.

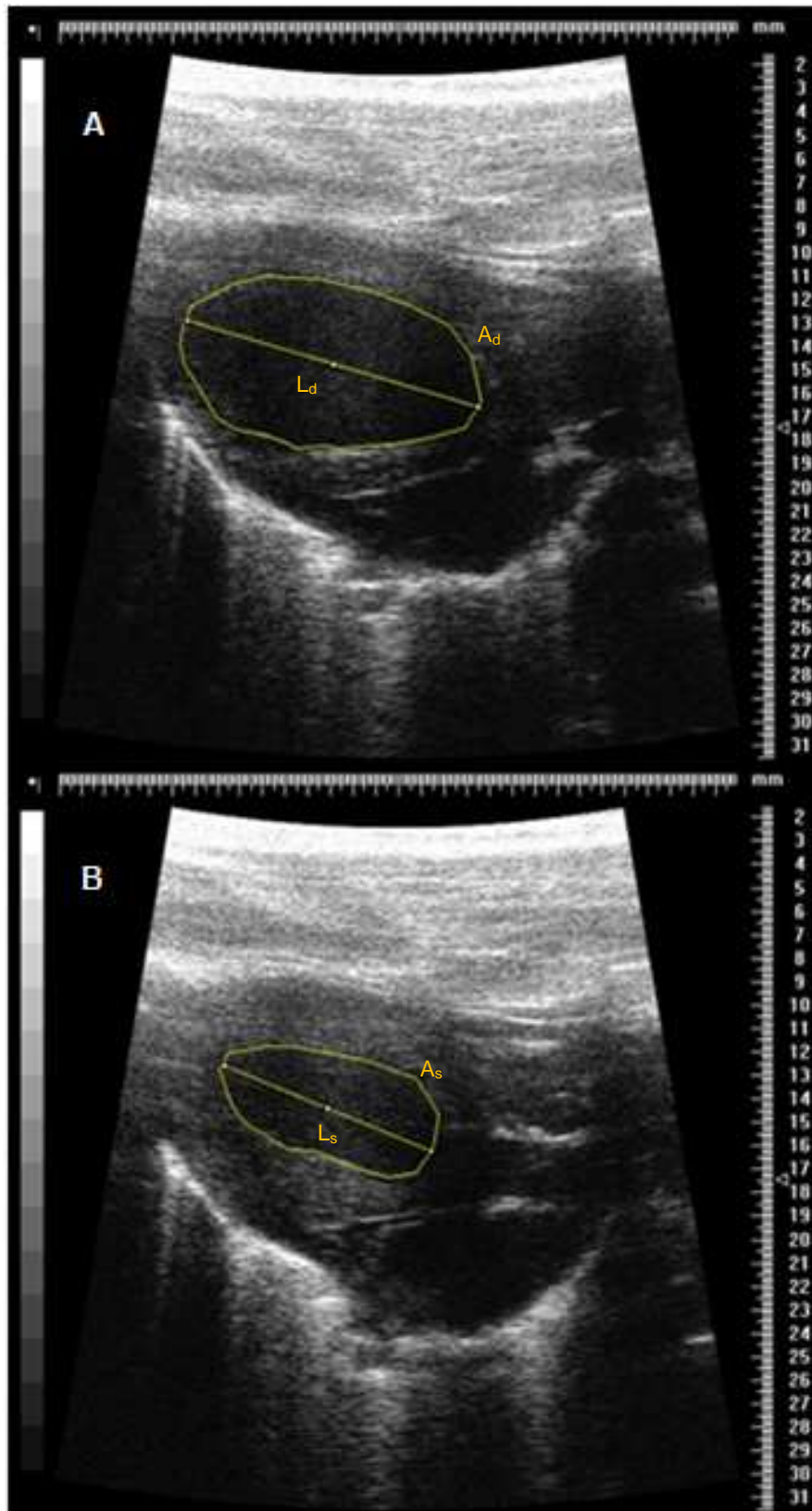


Figure 9: Diastolic and systolic left ventricular measurements. LV area and major axis are determined in parasternal long axis view during diastole (A) and systole (B). Both measurements from the same cardiac cycle and the same movie figure 6 was taken.

All measurements and calculations are made over three consecutive cardiac cycles, and the average ejection fraction determined.

3.3. Optical Mapping

Optical mapping of the rat heart is performed to visualize the electrical activity of the heart, specifically in and around the infarcted zone, in order to better assess the degree of cardiac regeneration when treated with HBM or saline. This is done by recording the signals of voltage sensitive fluorescent dyes and subsequent evaluation of these signals.

3.3.1. Harvest of heart

After the last echocardiography assessment, 8 weeks post MI, the rat is sacrificed and its heart harvested. For this, the animal is anesthetized with 2.5% Isoflurane. When no more signs of pain or other reactions are exhibited (e.g. after pinching the tail and paws), 2.0 ml of Heparin (45 IU/ml) are injected I.P. After approximately five minutes and testing the pain reflexes once more, the surgery is started. The ribcage is opened on both sides and the resulting flap is folded over the head of the animal to give better access to the heart. The heart is removed and care is taken to not damage the heart or cut the aorta too close to the heart. Once all vessels are cut, the heart is placed in previously prepared, ice cold Tyrode's solution (Table 1). Any unnecessary tissue that might still be attached to heart is removed, and the aorta is cannulated with a cannula made from a 15 gauge needle. Right cannulation of the aorta is confirmed by pumping Tyrode's solution dyed with food coloring through the cannula and observing the discoloration of the coronary arteries. Once cannulation is complete, the heart is immediately placed in the life support system (LSS).

Table 1: Composition of Tyrode's solution.

| Ingredient | Amount [mM] |
|---|--------------------|
| NaCl | 128.2 |
| KCl | 4.7 |
| NaHCO ₃ | 20 |
| CaCl ₂ | 1.3 |
| NaHPO ₄ | 1.19 |
| MgCl ₂ | 1.05 |
| D-Glucose | 10.1 |
| Oxygenated with 95% O ₂ / 5% CO ₂ | |

3.3.2. Life support system and image acquisition

After the harvest, the heart is placed in the LSS and retrograde perfused through the cannulated aorta. This causes perfusate (Tyrode's solution) to enter the coronary arteries and supply the myocardium with nutrients and oxygen, thus being able to keep it alive for hours outside the body. The LSS is comprised of chamber where the heart is placed in, three peristaltic pumps operating the flow to the cannula, to and from the chamber, two water baths heating the perfusate entering the cannula and water bath + two temperature probes measuring these, and a pressure probe measuring the pressure at which perfusate enters the cannula (Figure 8). The temperature in the cannula and chamber are kept at $37\pm 1^\circ\text{C}$, and the pressure between 50-80 mmHg. The pressure is adjusted by changing the flow rate to the cannula, but is started out at 5-6 ml/min. Once the heart is placed in the LSS and correctly perfused, the voltage sensitive dye Di-4-ANEPPS (Invitrogen) is added. 15 μl of dye stock solution (5mg Di-4-ANEPPS in 5ml DMSO) are mixed with 5 ml Tyrode's solution and injected into the perfusate upstream of the cannula to allow slower entry into the heart. Stimulation (3-4 Hz, 10-20 V, 6 ms duration) is added by placing one electrode in the water bath and one on the epicardium. Then the heart is illuminated with green laser light at a wavelength of 532 nm. The laser light first passes through a 5° diffuser and then reaches a dichroic mirror where it is reflected onto the heart.

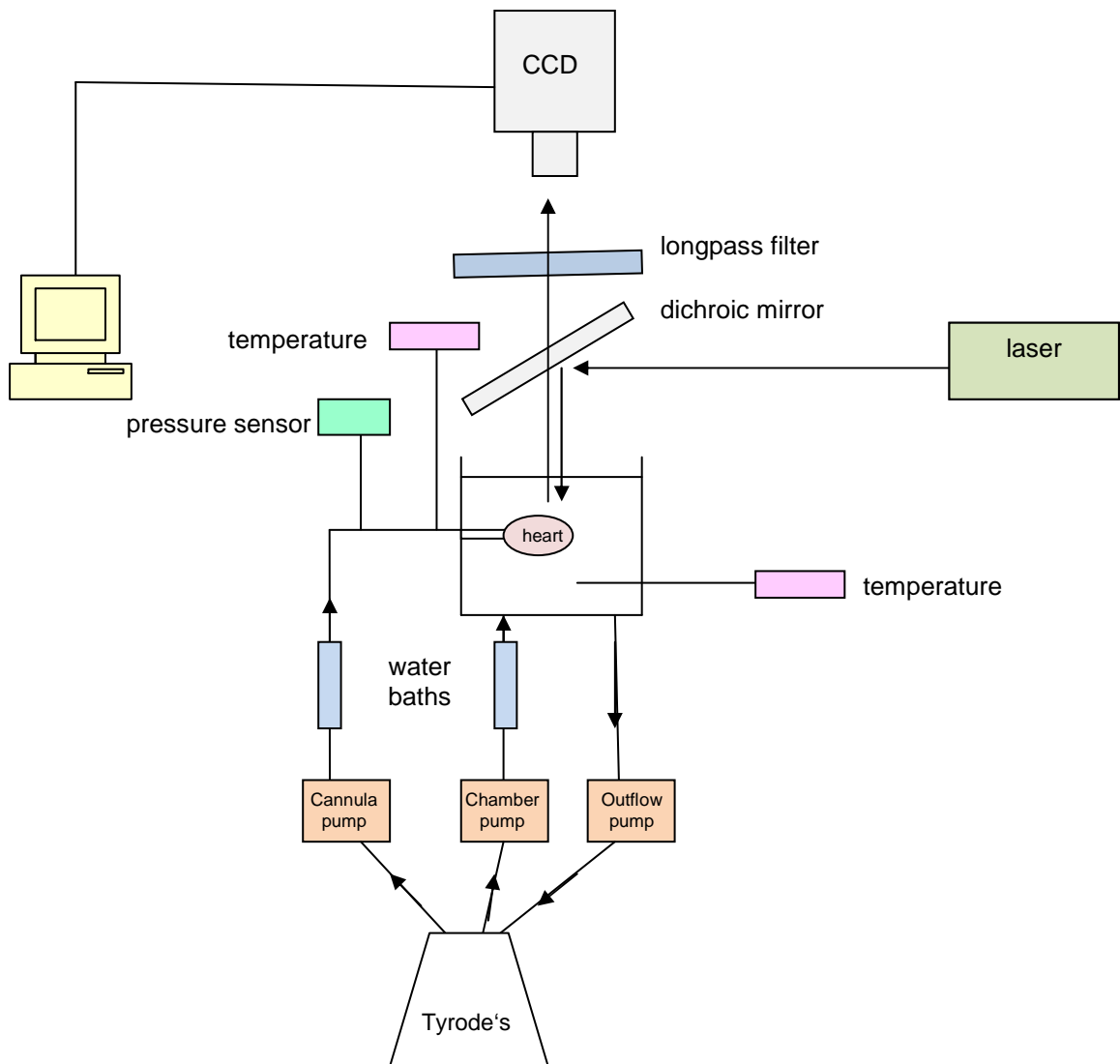


Figure 10: Schematic drawing of the optical mapping set up. Peristaltic pumps are used to circulate Tyrode's solution. Before entering the chamber and cannula, the solution passes through a water bath. The temperature and pressure with which solution enters the cannula is measured and the flow rate adjusted accordingly. The temperature of the solution entering the cannula and in the water bath is monitored and regulated with the water baths. The laser illumination arrives at the dichroic mirror, where it is reflected onto the heart. The emitted fluorescence light passes through the dichroic mirror and is filtered by a long pass filter, which allows only light above a certain wavelength to pass. The images collected by the CCD camera are sent to a computer, where they can be analyzed with the specially written program.

The light emitted by the fluorescent dye passes through the dichroic mirror without being reflected because it is of higher wavelength ($>567\text{nm}$), and through a 715 nm long pass filter. The long pass filter lets only light of a wavelength higher than 715 nm pass. The filtered light then reaches the objective of the charge coupled

device (CCD) based camera (SciMeasure). The camera transmits the received signal to a connected computer with a specifically developed program that displays the recordings and collected signals over 1000 frames and 80x80 pixels.

3.3.3. Signal evaluation

To analyze the signal received from the CCD camera, the described program its different functions for signal filtering are used. In order to assess the electrical activity in the infarct zone, the activation map is used as it displays the activation propagation and any irregularities in the propagation. The automated program for the activation signal works as described below:

The starting signals are the raw fluorescence signals as recorded by the camera over 1000 frames and 80x80 pixels. This signal is averaged over space and time, the minimum value is subtracted and then flipped. Then the program determines the maximum and minimum intensity over all pixels and uses it to find the minimal value for an upstroke to be the start of an activation potential. After determining this, it finds all activation potentials that occur over all pixels, and remembers the start and end frame plus a certain range of the strongest one. Criteria for an action potential are that the upstroke meets the minimal value, and that the upstroke occurs in a certain frame range. After having found the best activation potential, the pixels are evaluated in the saved frame range and the frame at which the minimum value for activation is reached is again saved for each pixel. Now, each pixel is assigned a shade of grey based on the time when activation occurred for this pixel. The grayscale is determined by using the earliest and latest activation time as reference points. The grey shades of each pixel are then plotted on a graph, resulting in the activation map, where black represents the earliest activation and white the latest. In addition to this automated process, an option has been added that allows excluding pixels that would influence the activation map in a bad way. This is done by setting a minimal difference between the maximum and minimum intensity, which makes it possible to exclude pixels with very low intensity to begin with. This value can be changed, and the effect on the activation map can be observed immediately.

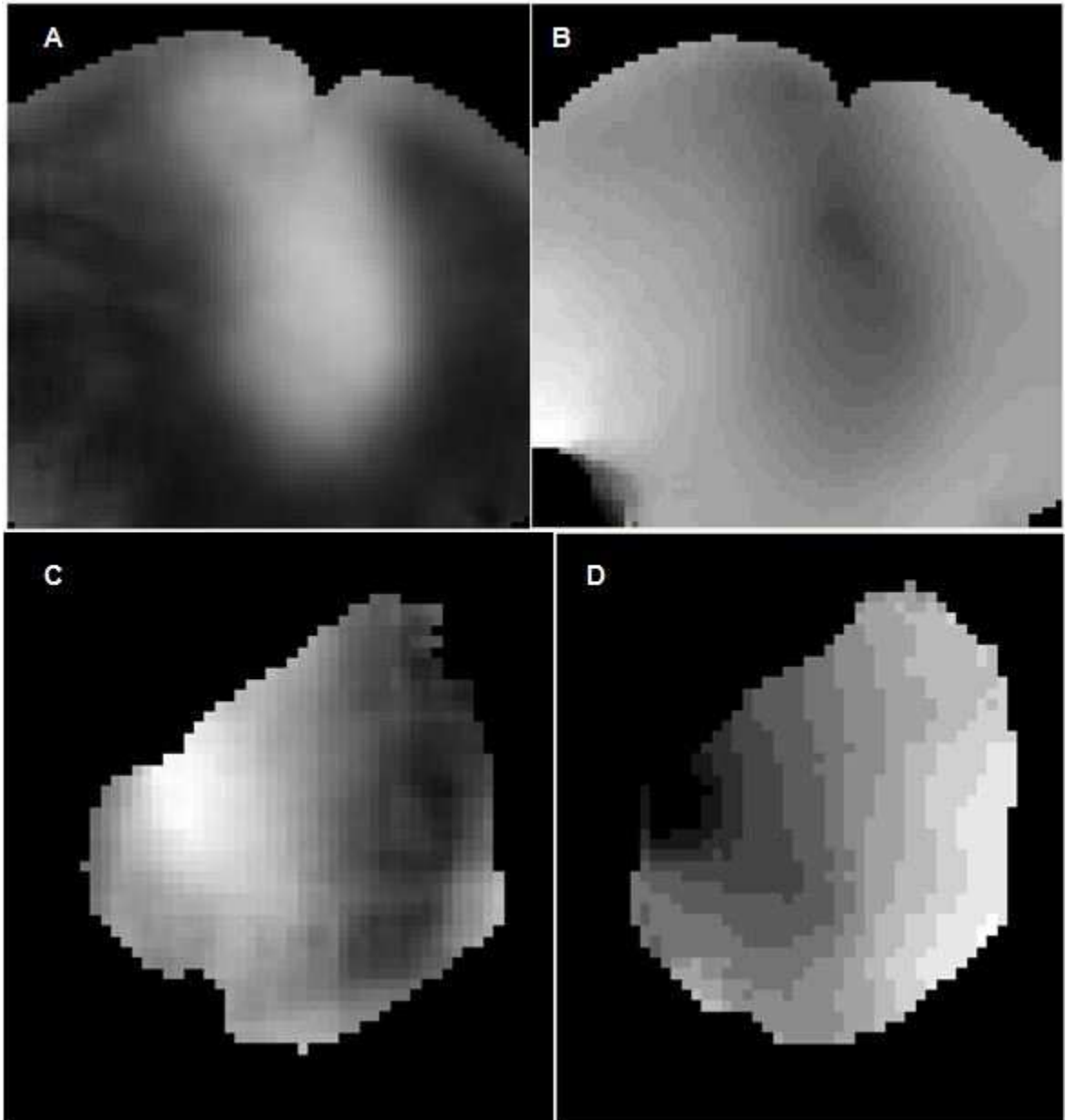


Figure 11: Image of stretched signal compared to activation map. (A)+(B) rabbit heart. (C)+(D) mouse heart. (A)+(C): image of stretched signal in mid-activation showing the propagation of the activation potential (white: high intensity, black low intensity). (B)+(D): automatically created activation map showing the different times when activation threshold was reached (black: earliest activation, white: latest activation).

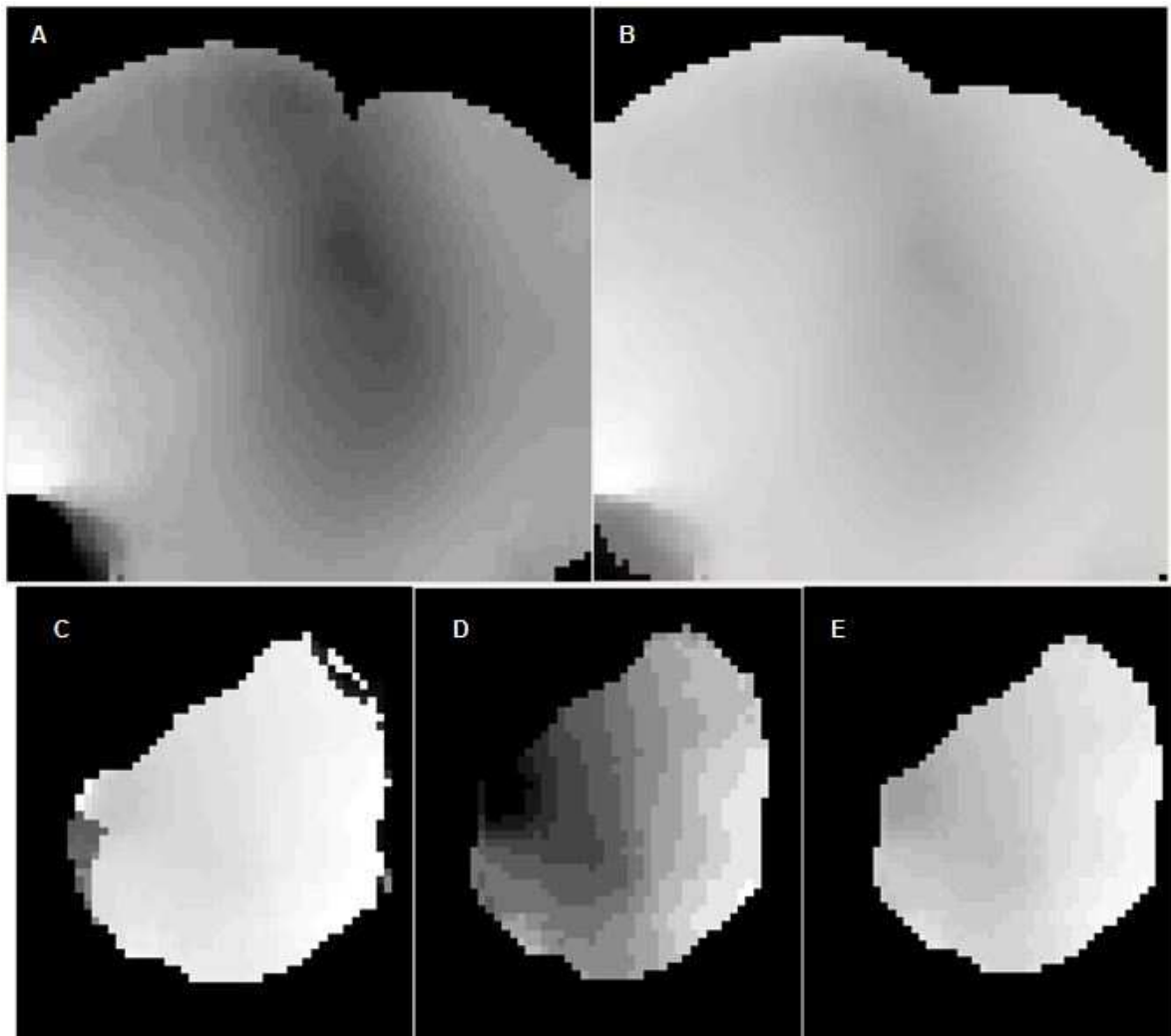


Figure 12: Effect of parameter change on activation map Images show the effect of changing the minimum amplitude range and the activation radius. **(A)+(B)** rabbit heart. **(C-E)** mouse heart. **(A)+(B)** have the same activation radius, but in **(A)** the minimum amplitude range is higher, thus excluding more pixels. **(C)+(D)** share the same minimum amplitude range, but in **(C)** the activation radius is much wider. **(D)+(E)** have the same activation radius, but the minimum amplitude range is 60 in **(D)** and 59 in **(E)**.

4. Discussion

For the treatment of myocardial infarction and subsequent heart failure, a new biomaterial, human basement membrane, is being tested. In order to assess the effect of HBM, myocardial infarction is induced in rats by ligation of LAD followed by the injection of HBM into the infarcted area. Cardiac function and regeneration is then evaluated with the use of echocardiography which is performed before the MI surgery, 4 weeks and 8 weeks post surgery. To determine the degree of electrical activity present in the infarcted and regenerated myocardium, optical mapping with the use of voltage sensitive fluorescent dyes is conducted. The focus of this paper is the development of the methods mentioned above.

For induction of MI, ligation of the LAD is a common method and has been used by several other groups^{22,23,53} investigating the effect of biomaterials on myocardial infarction. In general, the surgical procedure used in this study is very similar to the ones described in other biomaterial studies, with only a few changes. The drugs Ketamine and Xylazine are often used as sedatives and anesthetics, but since Xylazine is known to induce bradycardia or sinus arrhythmia⁵⁴, it was decided to use Midazolam instead. However, after the death of one animal due to unclear reasons, the use of drugs (Amiodarone, Phenylephrine, Ketamine and Midazolam) has been omitted. Omission of these drugs during the following surgery did not lead to any unwanted events so they have not been used again. In some cases the anesthesia provided by Isoflurane is not enough to completely suppress nerve reactions, which is when small amounts of Ketamine are administered. Tracheostomy has been used as the intubation method of choice because it provides a definite way of intubating the trachea, and not accidentally the esophagus which was the case with oro-tracheal intubation. Since the esophagus and the trachea are very close together, and the esophagus is very thin, it was possible to feel the typical tracheal rings even when the intubation tube was in the esophagus. This led to the assumption of animal being correctly intubated even if this was not the case. One drawback of using tracheostomy is that it creates another surgical site that needs to be closed and is a potential site for infection. Furthermore, closing the trachea after the endo-tracheal tube is removed may

cause difficulties, too. Unfortunately, with this study's budget it was not possible to buy blood pressure and ECG measuring systems appropriate for rodents. Even though being able to observe the blood pressure could be of use, so far it has not been a necessity, especially after omitting the blood pressure affecting drugs Amiodarone and Phenylephrine. Unlike the blood pressure reading, obtaining good ECG readings was definitely necessary. This problem has been solved by using a DC amplifier to amplify the signals detected with alligator clip electrodes and an oscilloscope to display the amplified signals. This set up is not capable of providing a heart rate in numbers, but the ECG signals are clearly distinguishable, and any changes in the waveform are easily detectable. One important change in waveform is the elevation of the ST- segment after LAD elevation. This ST segment elevation is characteristic for the early phase of a myocardial infarction⁶ and is also used as an MI indicator by other groups^{3,22}. The specially modified needle for the injection of HBM or saline into the infarct, as seen in figure 5, has also proven to be very useful. Due to the high heart rate in rats (~300 beats per minute), any injection into the heart can be very difficult. After measuring the LV wall thickness in a rat heart (~3mm), a 30ga needle was cut to about half of the wall thickness to reduce the risk of accidentally damaging the heart. Even though this injection could also be made with a normal needle, this special needle definitely simplifies it.

Echocardiography is another method that has been used in similar studies²³. It allows the assessment of cardiac function by measuring and calculating different parameters. In this case, ejection fraction is being used as the major determinant of cardiac function. Most commonly, one dimensional M-mode readings are used for this, as they display the LV change over time (figure 13).

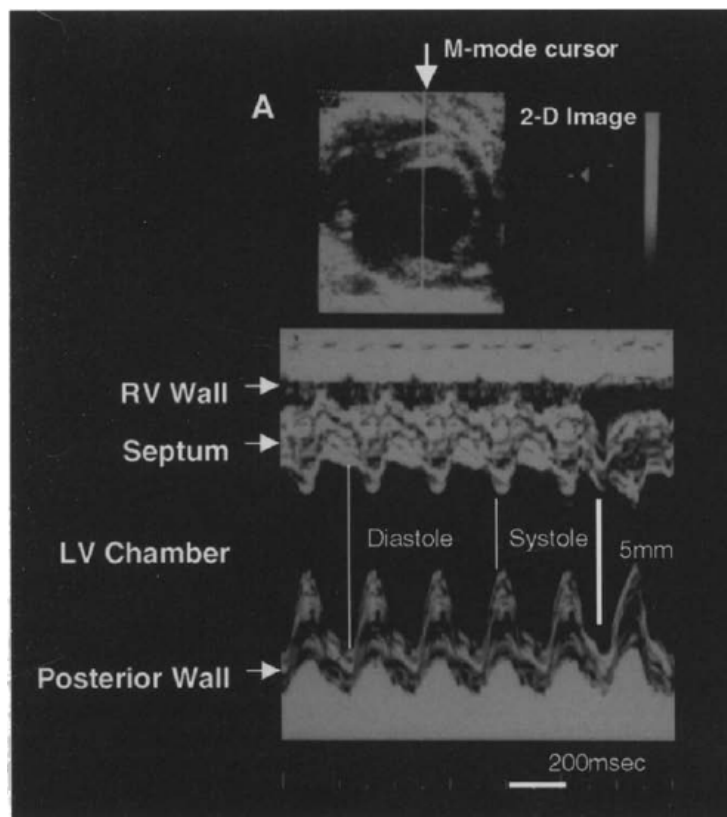


Figure 13: M-mode image through parasternal short axis view of the heart. Modified after⁴⁵

However, due to the one dimensionality of those measurements and that any calculations thereof are based on the assumption of symmetrical geometry of the LV⁴², this method is more prone to error than two dimensional views⁴⁵, especially in MI studies where LV remodeling can alter the shape of the LV. Therefore, two dimensional views have been selected as view of choice in this study, but also other groups used 2D views rather than 1D for their measurements⁴¹. The ejection fraction can be calculated from parasternal long axis or apical views⁴⁴, and since PLA images can be easily obtained, we decided for this view. The PLA image we obtain from echocardiography show the left ventricle when it's at its largest. The left atrium and aorta should be visible as well (figure xx). In order to calculate the ejection fraction, diastolic and systolic volumes have to be calculated. After reading through several papers and different ways to calculate the volume from 2D images, this formula $V_{d/s} = 0.85 \frac{(A_{d/s})^2}{L_{d/s}}$ has been decided on^{44,52}, as it is most

compatible with the ellipsoid shape of the LV in parasternal long axis view. There are also other formulas and volume measurement techniques that are being used by some groups^{55,56}, but neither of those seemed to fit our purpose and the view we chose to use. As can be seen from the formula, ventricular area and length of major axis have to be measured first, both during systole and diastole, as we did in figure xx. The left ventricular inner wall is traced to obtain the area, and the major axis is measured from the apex to the aortic valve. This figure also shows the volume changes between diastole and systole very well. Ideally, the information obtained with echocardiography should show that the treatment with HBM results in better ejection fraction, and thus improved cardiac function.

The procedure used to harvest the heart is a routine procedure used also for other animal species in Dr. Zemlin's group. With the exception of the heparin concentration and the size of the cannula, the steps are the same. Heparin is an anti-coagulant and serves the purpose of preventing the formation of blood clots in the heart, which can cause severe damage. When removing the heart, it is important not to cut the aorta too close to the heart, as this will complicate the cannulation process immensely. It is also important that the Tyrode's solution in which the heart is placed after its removal is ice cold to slow the metabolism until the heart can be placed in the LSS. This life support system uses a chamber that is filled with Tyrode's solution, but also other set ups can be used that not always utilize any chambers⁵⁷. For visualization of the electrical activity in the heart, the voltage sensitive dye Di-4-ANEPPS is used. This dye belongs to the family of electrochromic dyes, which means that the dye exhibits a wavelength shift upon polarization^{51,58}. The excitation range for Di-4-ANEPPS is between 450 and 550 nm, so a green laser with a wavelength of 532 nm is used. The green laser light is on the edge of the excitation range, but due to the electrochromic property of the dye, this results in a better detectable wavelength shift upon polarization. The emission spectrum of Di-4-ANEPPS ranges from about 510-850nm (figure 14). The first filter barrier is the dichroic mirror that reflects any light with a wavelength below 567nm. The long pass filter only allows light with a wavelength greater than 715 nm to pass. This assures that only light emitted by the fluorescent dye is

captured. A schematic drawing of the complete optical mapping setup is shown in figure 8.

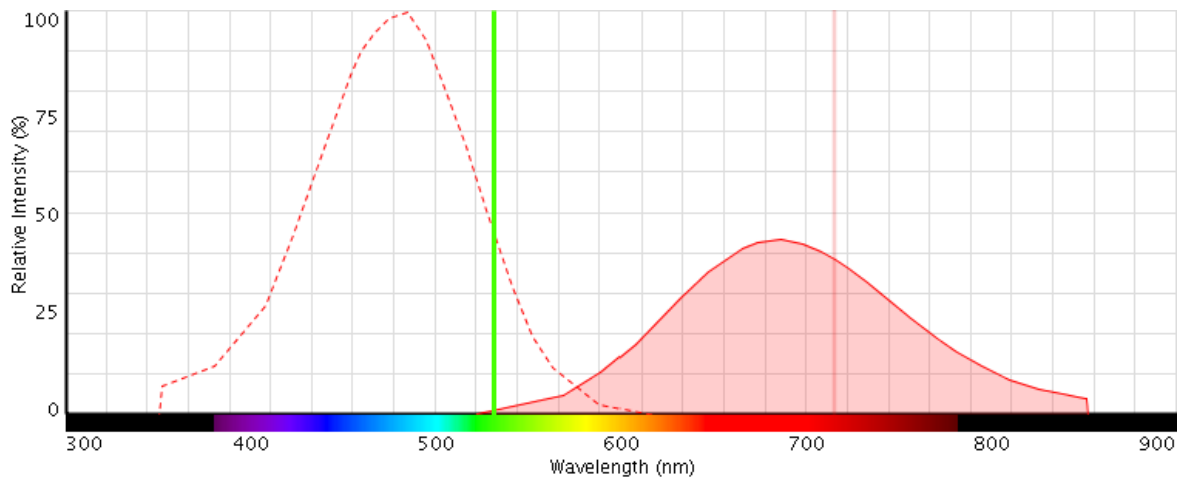


Figure 14: Excitation/emission spectrum of Di-4-ANEPPS. The dotted line shows the excitation spectrum of Di-4-ANEPPS. The green line represents the used laser (532 nm). The red curve shows the emission spectrum and its intensity when excited at this wavelength. The vertical red line at 715nm represents the long pass filter. All light with a wavelength above this vertical line is being collected. Graph created with Fluorescence SpectraViewer⁵⁹

The user interface of the program used to analyze the images and fluorescent signals recorded by the CCD camera provides images of the raw image, an activation or action potential duration map, and the fluorescence signal with respect to time (figure xx). It is possible to filter the image in several different ways, create action potential duration maps, amplitude maps and activation maps as well as change the parameters for creating these maps. The most used filters are the time running average, space running average, subtraction of minimum amplitude and flipping as well as stretching the image filtered in this way. The thus resulting effect on the signal can be seen in figure 10, where it is demonstrated on a rabbit and a mouse heart. The signals from the rabbit heart (figure 10 **A-C**) very nicely show flipping makes the action potential appear as an upstroke. Especially the mouse signals (figure 10 **D-F**) emphasize how the filtering steps can enhance the fluorescent signal, as they are noisier than the rabbit signals. **B/C** and **E/F** are filtered in the same way except that the signal in **C** and **F** has been stretched to the maximum intensity which results in a visible output picture. In this output

picture one is able to see the propagation of the action potential when moving through the frames. In these pictures, white means high intensity, black low intensity, and as each pixels action potential starts at a slightly different time point, the action potential spreads as a white wave, starting at the point of stimulation.

An activation map is basically a static image of the action potential propagation. While the stretched signal image only shows the intensity in each pixel at only one, the activation map colors each pixel according to the frame number at which the previously set activation threshold is reached. Black means the activation threshold is reached at an early frame while white means later activation. Even though both images, stretched image and activation map, show slightly different things, they tell the same information: where the activation starts and how it is travelling across the heart. This is shown very well in figure 11, where the stretched image and the activation map of a rabbit heart (figure 11 **A+B**) and mouse heart (**C+D**) are seen next to each other. Despite the flipped colors and different mechanism, the start of activation/propagation is clearly visible in all four images.

How important it is to use the right parameters for the creation of the activation map is seen in figure **xx** where the activation maps were created from the same two movies, but with a changed minimum amplitude and activation radius. When the activation map is created, the program looks in each pixel if the activation threshold is reached and saves the frame at which this occurs for each pixel. The frame range in which the program does this can be changed with the setting "Activation Radius". The program also excludes pixels for the activation map if their difference between maximum and minimum amplitude is below a certain level. Otherwise pixels whose signal is very low and might not follow the rest of the tissue's pattern could compromise the activation map by either having a very late or very early activation frame. This minimum difference can also be changed. **A+B** in figure 12 show activation maps created with different minimum differences. A has a higher minimum difference, causing more pixels to be excluded and thus fewer frames where activation occurs. The difference between the maps seen in figure 10 **C** and **D** is the activation radius. Since the form of the activation potential

in mice is much narrower than that in rabbits (figure 10), the range in which the program looks for activation should be much narrower too. Figure 10 **C** has wider activation radius than **D**. Between figure 10 **D** and **E**, the only difference is again the minimum difference. In **D**, the value was set to 60; in **E** it was set to 59, so even very small steps can have a great impact, which is why it's important to check the set parameters carefully. All this is not possible in the previous program used for the creation of activation maps. There, it was necessary to apply all filters manually, and check the pixels for a suitable action potential upstroke. The frame range in which the program looked for activation was then set manually. Compared to the automatically created activation map, the maps were often smaller and the map didn't span across the whole heart or pixels with bad signals were not excluded which negatively influenced the color distribution. In figure **xx** this difference can be seen very clearly. Both maps have been created from the exact same starting signal.

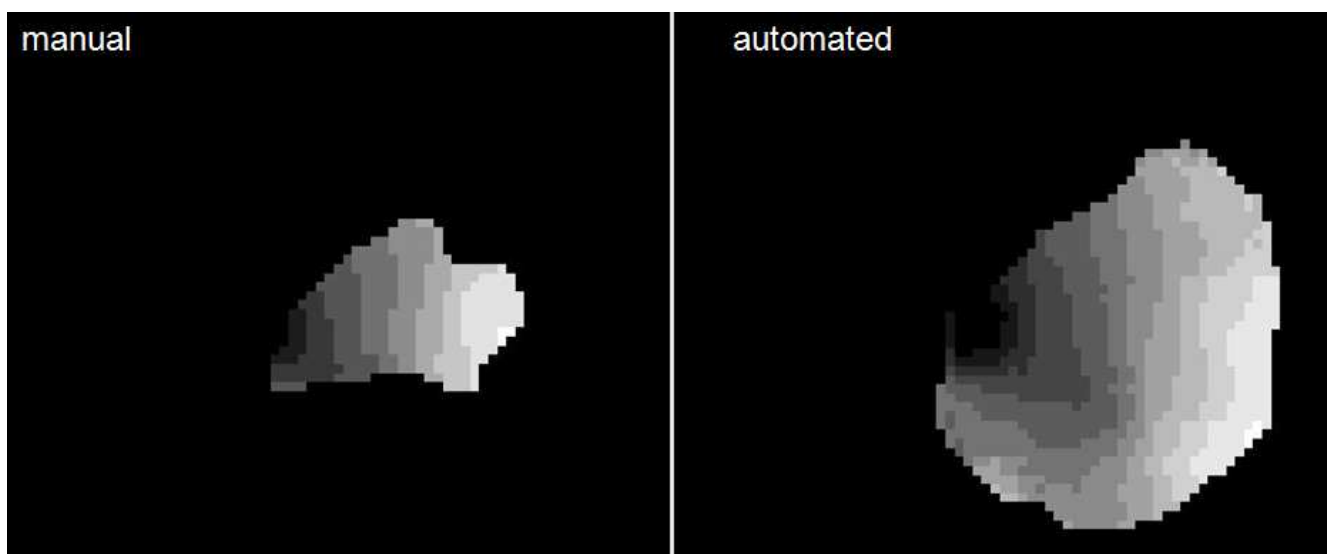


Figure 15: Manually and automatically created activation map. The activation map that was created by manually selecting the frame range shows a much smaller activation map than compared to the automatically created one, which spans across the whole heart.

These maps and the way they can be enhanced should enable us to distinguish the infarcted zones from the non-infarcted zones in the rat hearts. Furthermore, we should be able to assess whether the electrical activity in the infarct zones of rats treated with HBM is different to the ones treated with only saline.

All methods together enable the group of Dr. Zemlin to determine whether HBM has any effect on the regeneration of cardiac tissue after myocardial infarction, and if yes, to what extent. Should it be the case that the biomaterial human basement membrane does have a positive effect on infarcted hearts another animal study with a bigger scope will be conducted. Eventually, the goal is to provide a novel treatment for myocardial infarction, and thus save or prolong the life of many patients.

5. References

1. Deaths from coronary heart disease. *WHO* at http://www.who.int/cardiovascular_diseases/en/cvd_atlas_14_deathHD.pdf
2. Zafari, M. A., Reddy, S. V, Jeroudi, A. M., Garas, S. M. & Yang, E. H. Myocardial Infarction. *MedScape* (2014). at <http://emedicine.medscape.com/article/155919-overview#a0156>
3. The Joint European Society of Cardiology/American College of Cardiology Committee. Myocardial infarction redefined--a consensus document of The Joint European Society of Cardiology/American College of Cardiology Committee for the redefinition of myocardial infarction. *Eur. Heart J.* **21**, 1502–13 (2000).
4. Widmaier, E. P., Raff, H. & Strang, K. T. in *Vander's Hum. Physiol. - Mech. Body Funct.* 405–417 (McGraw Hill, 2011).
5. Swirski, F. K. & Nahrendorf, M. Leukocyte behaviour in atherosclerosis, myocardial infarction, and heart failure. *Science (80-.)*. **339**, 161–166 (2013).
6. Netter, F. H. in *Farbatlanten der Medizin - Ciba Collect. Med. Illus.* 38–144 (Georg Thieme Verlag, 1990).
7. Gaudron, P., Eilles, C., Kugler, I. & Ertl, G. Progressive left ventricular dysfunction and remodeling after myocardial infarction. Potential mechanisms and early predictors. *Circulation* **87**, 755–763 (1993).
8. Venugopal, J. R. *et al.* Biomaterial strategies for alleviation of myocardial infarction. *J. R. Soc. Interface* **9**, 1–19 (2012).
9. Phinikaridou, A., Andia, M. E., Shah, A. M. & Botnar, R. M. Advances in molecular imaging of atherosclerosis and myocardial infarction: shedding new light on in vivo cardiovascular biology. *Am. J. Physiol. Heart Circ. Physiol.* **303**, H1397–410 (2012).
10. Leor, J., Amsalem, Y. & Cohen, S. Cells, scaffolds, and molecules for myocardial tissue engineering. *Pharmacol. Ther.* **105**, 151–63 (2005).
11. St John Sutton, M. & Ferrari, V. a. Prevention of Left Ventricular Remodeling After Myocardial Infarction. *Curr. Treat. Options Cardiovasc. Med.* **4**, 97–108 (2002).
12. Christman, K. L. & Lee, R. J. Biomaterials for the treatment of myocardial infarction. *J. Am. Coll. Cardiol.* **48**, 907–13 (2006).

13. Rane, A. a & Christman, K. L. Biomaterials for the treatment of myocardial infarction: a 5-year update. *J. Am. Coll. Cardiol.* **58**, 2615–29 (2011).
14. St John Sutton, M. *et al.* Left ventricular remodeling and ventricular arrhythmias after myocardial infarction. *Circulation* **107**, 2577–82 (2003).
15. Minicucci, M. F., Azevedo, P. S., Polegato, B. F., Paiva, S. a R. & Zornoff, L. a M. Heart failure after myocardial infarction: clinical implications and treatment. *Clin. Cardiol.* **34**, 410–4 (2011).
16. Chachques, J. C. *et al.* Myocardial Assistance by Grafting a New Bioartificial Upgraded Myocardium (MAGNUM trial): clinical feasibility study. *Ann. Thorac. Surg.* **85**, 901–8 (2008).
17. Ott, H. C. *et al.* Perfusion-decellularized matrix: using nature's platform to engineer a bioartificial heart. *Nat. Med.* **14**, 213–21 (2008).
18. Radisic, M. & Christman, K. L. Materials science and tissue engineering: repairing the heart. *Mayo Clin. Proc.* **88**, 884–98 (2013).
19. Christman, K. L. *et al.* Injectable fibrin scaffold improves cell transplant survival, reduces infarct expansion, and induces neovasculature formation in ischemic myocardium. *J. Am. Coll. Cardiol.* **44**, 654–60 (2004).
20. Ryu, J. H. *et al.* Implantation of bone marrow mononuclear cells using injectable fibrin matrix enhances neovascularization in infarcted myocardium. *Biomaterials* **26**, 319–26 (2005).
21. Dai, W., Wold, L. E., Dow, J. S. & Kloner, R. a. Thickening of the infarcted wall by collagen injection improves left ventricular function in rats: a novel approach to preserve cardiac function after myocardial infarction. *J. Am. Coll. Cardiol.* **46**, 714–9 (2005).
22. Ou, L. *et al.* Intracardiac injection of matrigel induces stem cell recruitment and improves cardiac functions in a rat myocardial infarction model. *J. Cell. Mol. Med.* **15**, 1310–8 (2011).
23. Landa, N. *et al.* Effect of injectable alginate implant on cardiac remodeling and function after recent and old infarcts in rat. *Circulation* **117**, 1388–96 (2008).
24. Wall, S. T., Walker, J. C., Healy, K. E., Ratcliffe, M. B. & Guccione, J. M. Theoretical impact of the injection of material into the myocardium: a finite element model simulation. *Circulation* **114**, 2627–35 (2006).
25. Zhang, Z. *et al.* Comparison of Young LaPlace law and infinite element based calculation of ventricular wall stress: Implications for post infarct surgical ventricular remodeling. *Ann Thorac Surg* **91**, 150–156 (2011).

26. Kamelger, F. . *et al.* A comparative study of three different biomaterials in the engineering of skeletal muscle using a rat animal model. *Biomaterials* **25**, 1649–1655 (2004).
27. Smits, P. C. *et al.* Catheter-Based intramyocardial injection of autologous skeletal myoblasts as a primary treatment of ischemic heart failure. *J. Am. Coll. Cardiol.* **42**, 2063–2069 (2003).
28. Krupnick, A. S. *et al.* A Novel Small Animal Model of Left Ventricular Tissue Engineering. *J. Hear. Lung Transplant.* **2498**, 233–243 (2002).
29. Rowe, R. G. & Weiss, S. J. Breaching the basement membrane: who, when and how? *Trends Cell Biol.* **18**, 560–74 (2008).
30. Yurchenco, P. D., Amenta, P. S. & Patton, B. L. Basement membrane assembly, stability and activities observed through a developmental lens. *Matrix Biol.* **22**, 521–38 (2004).
31. Kruegel, J. & Miosge, N. Basement membrane components are key players in specialized extracellular matrices. *Cell. Mol. Life Sci.* **67**, 2879–2895 (2010).
32. Kleinman, H. K. & Martin, G. R. Matrigel: basement membrane matrix with biological activity. *Semin. Cancer Biol.* **15**, 378–386 (2005).
33. Laflamme, M. a *et al.* Cardiomyocytes derived from human embryonic stem cells in pro-survival factors enhance function of infarcted rat hearts. *Nat. Biotechnol.* **25**, 1015–24 (2007).
34. Baharvand, H., Azarnia, M., Parivar, K. & Ashtiani, S. K. The effect of extracellular matrix on embryonic stem cell-derived cardiomyocytes. *J. Mol. Cell. Cardiol.* **38**, 495–503 (2005).
35. Leri, A., Kajstura, J., Anversa, P. & Frishman, W. H. Myocardial regeneration and stem cell repair. *Curr. Probl. Cardiol.* **33**, 91–153 (2008).
36. Klocke, R., Tian, W., Kuhlmann, M. T. & Nikol, S. Surgical animal models of heart failure related to coronary heart disease. *Cardiovasc. Res.* **74**, 29–38 (2006).
37. Patten, R. D. & Hall-Porter, M. R. Small animal models of heart failure: development of novel therapies, past and present. *Circ. Heart Fail.* **2**, 138–44 (2009).
38. Goldman, S. & Raya, T. E. Rat infarct model of myocardial infarction and heart failure. *J. Card. Fail.* **1**, 169–77 (1995).

39. Pfeffer, M. a *et al.* Myocardial infarct size and ventricular function in rats. *Circ. Res.* **44**, 503–12 (1979).
40. Pfeffer, M. a, Braunwald, E., Basta, L., Brown, E. J. & Davis, B. R. *et al.* Effect of captopril on mortality and morbidity in patients with left ventricular dysfunction after myocardial infarction. *N. Engl. J. Med.* **327**, 669–677 (1992).
41. Sjaastad, I., Sejersted, O. M., Ilebekk, a & Bjornerheim, R. Echocardiographic criteria for detection of postinfarction congestive heart failure in rats. *J. Appl. Physiol.* **89**, 1445–54 (2000).
42. Gottdiener, J. S. *et al.* American Society of Echocardiography recommendations for use of echocardiography in clinical trials. *J. Am. Soc. Echocardiogr.* **17**, 1086–119 (2004).
43. Brown, L. *et al.* Echocardiographic assessment of cardiac structure and function in rats. *Heart. Lung Circ.* **11**, 167–73 (2002).
44. Stypmann, J. *et al.* Echocardiographic assessment of global left ventricular function in mice. *Lab. Anim.* **43**, 127–37 (2009).
45. Coatney, R. W. Ultrasound imaging: principles and applications in rodent research. *ILAR J.* **42**, 233–47 (2001).
46. Rosenbaum, D. S. in *Opt. Mapp. Card. Excit. Arrhythm.* (Rosenbau, D. & Jalife, J.) 2–7 (2001).
47. Herron, T. J., Lee, P. & Jalife, J. Optical Imaging of Voltage and Calcium in Cardiac Cells & Tissue. *Circ. Res.* **110**, 609–623 (2012).
48. Sill, B., Hammer, P. E. & Cowan, D. B. Optical mapping of Langendorff-perfused rat hearts. *J. Vis. Exp.* 2–5 (2009). doi:10.3791/1138
49. Efimov, I. R., Nikolski, V. P. & Salama, G. Optical Imaging of the Heart. *Circ. Res.* **95**, 21–33 (2004).
50. Fast, V. G. Simultaneous optical imaging of membrane potential and intracellular calcium. *J. Electrocardiol.* **38**, 107–12 (2005).
51. Loew, L. M. in *Membr. Potential Imaging Nerv. Syst. Methods Appl.* (Canepari, M. & Zecevic, D.) 13–23 (Springer New York, 2011). doi:10.1007/978-1-4419-6558-5
52. Article, S. Standard measurement of cardiac function indexes. *J. Med. Ultrason.* **33**, 123–127 (2006).

53. Li, X.-H. *et al.* Effects of intramyocardial injection of platelet-rich plasma on the healing process after myocardial infarction. *Coron. Artery Dis.* **19**, 363–70 (2008).
54. Hsu, W. ., Zheng-Xing, L. & Hembrough, F. B. Effect of xylazine on heart rate and arterial blood pressure in conscious dogs, as influenced by atropine, 4-aminopyridine, doxapram, and yohimbine. *J. Am. Vet. Med. Assoc.* **186**, (1985).
55. Brown, L. *et al.* Echocardiographic Assessment of Cardiac Structure and Function in Rats. *Hear. Lung Circ.* **11**, (2002).
56. Lang, R. M. *et al.* Recommendations for chamber quantification. *Eur. J. Echocardiogr.* **7**, 79–108 (2006).
57. Bell, R. M., Mocanu, M. M. & Yellon, D. M. Retrograde heart perfusion: the Langendorff technique of isolated heart perfusion. *J. Mol. Cell. Cardiol.* **50**, 940–50 (2011).
58. Loew, L. M. in *Opt. Mapp. Card. Excit. Arrhythm.* (Rosenbaum, D. S. & Jalife, J.) 33–46 (Wiley-Blackwell, 2001).
59. Fluorescence SpectraViewer. at <http://www.lifetechnologies.com/us/en/home/life-science/cell-analysis/labeling-chemistry/fluorescence-spectraviewer.html#product=D1199>
60. Echokardiographie. *www.deacademia.com - Acad. dictionaries Encycl.* at <http://de.academic.ru/dic.nsf/dewiki/368865>
61. Berndt, A., Leme, A., Paigen, B., Shapiro, S. & Svenson, K. MPD - Berndt2 - protocol. *Mouse Phenom Database Jackson Lab.* at http://phenome.jax.org/db/q?rtn=projects/docstatic&doc=Berndt2/Berndt2_Protocol
62. Zemlin, C. Heart Attacks | Electrophysiology. at <http://ww2.odu.edu/~czemlin/heartattacks.html>